INTERNATIONAL ATOMIC ENERGY AGENCY
UNITED NATIONS EDUCATIONAL, SCIENTIFIC AND CULTURAL ORGANIZATION

INTERNATIONAL CENTRE FOR THEORETICAL PHYSICS
34100 TRIESTE (ITALY) - P.O.B. 586 - MIRAMARE - STRADA COSTIERA 11 - TELEPHONES: 224281/2 3 4/5 6
CABLE: CENTRATOM - TELEX 460392-I

SMR/98 - 30

AUTUMN COURSE ON GEOMAGNETISM, THE IONOSPHERE
AND MAGNETOSPHERE

(21 September - 12 November 1982)

# WAVES AND WAVE-PARTICLE INTERACTIONS IN THE MAGNETOSPHERE.

Roger GENDRIN

Centre de Recherches en Physique de l'Environnement
Centre National d'Etudes des Télécommunications
3, avenue de la République
92131 Issy-les-Moulineaux
FRANCE

# WAVES AND WAVE-PARTICLE INTERACTIONS IN THE MAGNETOSPHERE

Lectures given at the Interrational Center for Theoretical Physics

Trieste, Italy, October 1982

by

Roger GENDRIN

Centre de Recherches en Physique de l'Environnement

Centre National d'Etudes des Télécommunications

3, avenue de la République, 92131 Issy-les-Moulineaux, France

## INTRODUCTION

## CHAPTER I

Appendix A



WAVES AND WAVE-PARTICLE INTERACTIONS IN THE MAGNETOSPHERE

Lectures given at the International Center for Theoretical Physics

Trieste, Italy, October 1982

by

Roger GENDRIN

Centre de Recherches en Physique de l'Environnement

Centre National d'Etudes des Télécommunications

3, avenue de la République, 92131 Issy-les-Moulineaux, France

## INTRODUCTION

The study of natural waves generated into and propagating through the magnetosphere is important for many reasons :

1. Although these waves do not transport a lot of energy (see below) they play a fundamental role by modifying the dynamics of magnetospheric particles (pitch angle or radial diffusion, acceleration, exchange of energy between different particle species) in an otherwise collisionless medium. Consequently their existence must be fully taken into account in any realistic model of almost all geophysical phenomena.

2. The study of these waves is equivalent to remotely sensing the plasma characteristics (density, temperature, composition, velocity distribution) of the regions where they are generated. This is valid only if one has the correct explanation of the mechanism by which they are generated. (One of the best example is the study of the decametric or metric radiation of Jupiter which yielded the values of the magnetic field intensity and of the energetic particle fluxes in the vicinity of this Planet well before any in situ measurement has confirmed more or less these values).

3. The deformation of the wave characteristics between the source region and the observing point gives also a valuable information on the properties of the medium through which the wave propagates. This information is usually an integrated value which in many cases (and under some realistic assumptions) can be transformed into a localized one. (One example is the deduction of the equatorial value of the cold plasma density in far regions of the magnetosphere made from the dispersion of whistlers four years before the first artificial satellite was launched).

Before starting the study of the different magnetospheric emissions, it is good to recall the definition of the different frequency ranges (Table 1). In this Table, a special column is reserved for the nomenclature of natural ULF magnetospheric signals (Chapters 1 and 2). Let us also give an idea of the spectral power of all these emissions, at least of the electromagnetic ones (Figure 1). It is possible to approximate the data presented in this Figure (Lanzerotti and Southwood, 1979)* by the formula

$$P \sim 10^{-7}/f^{1.7} \qquad (1)$$

where P is in $W.m^{-2}.Hz^{-1}$ and f in Hz. This power flux is rather small.

* *referenced to in Chapter 1*

*L.J. Lanzerotti and D.J. Southwood, Hydromagnetic Waves*
*in 'Solar System Plasma Physics', vol.3, 1979.*

Table 1
Classification of magnetospheric signals



| Name | Frequency | | Name | Period or rise time (secs) |
|---|---|---|---|---|
| SHF | 3–30 | GHz | Pc 1 | $2\pi/\omega$ = 0.2–5 |
| UHF | 0.3–3 | GHz | Pc 2 | $2\pi/\omega$ = 5–10 |
| VHF | 30–300 | MHz | Pc 3 | $2\pi/\omega$ = 10–45 |
| HF | 3–30 | MHz | Pc 4 | $2\pi/\omega$ = 45–150 |
| MF | 0.3–3 | MHz | Pc 5 | $2\pi/\omega$ = 150–600 |
| LF | 30–300 | kHz | | |
| VLF | 3–30 | kHz | Pi 1 | $\tau_r$ = 1–40 |
| ELF | 3–3000 | Hz | Pi 2 | $\tau_r$ = 40–150 |
| ULF | ≤3 | Hz | sc, si | $\tau_r$ ~300– |

*L.J. Lanzerotti and D.J. Southwood, Hydromagnetic Waves in 'Solar System Plasma Physics', vol.3, 1979.*

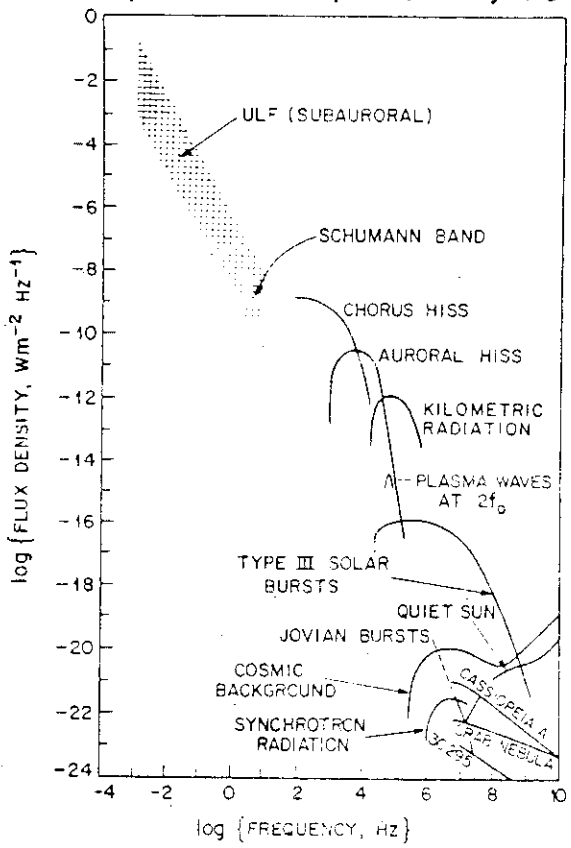


Fig. 1. Power flux levels for various frequency ranges of naturally-occurring waves in the Earth's environment and in astrophysical sources as observed at Earth.



For instance, the kilometric radiation ($10^{-12}$ $W.m^{-2}.Hz^{-1}$), integrated over a bandwidth of 100 kHz corresponds to a power flux of $10^{-7}$ $W.m^{-2}$. This has to be compared with the power flux deposited in the auroral zone by precipitating particles ($\sim$ 20-100 m $W.m^{-2}$)*, which is much more important. However the power fluxes which are reported in the literature have been usually measured far from the source region. What counts is the total power radiated, which depends on the geometrical dispersion of the waves. In the case of kilometric radiation for instance, Gurnett (1982)**, integrating over $2\pi$ quotes numbers between $10^7$ and $10^9$ W. When compared with the total kinetic power of precipitating particles during intense aurorae ($\sim 2 \times 10^{10}$-$10^{11}$ W)* the difference is not so large.

Similar comparisons can be made in different frequency ranges and the answers are always the same : the power which is contained in the waves is always smaller than (and often negligible with respect to) the power which is contained in the particles. However , this may not be always the case. For instance the hourly energy deposition by Joule heating from a strong pulsation event may be an appreciable fraction ($\sim$ 4%) of the total energy released during a weak substorm (Greenwald and Walker, 1980). Moreover, because of the possible annulation of the group velocity, the wave field may become very large. Then in a limited volume the wave energy density exceeds the particle energy density and non linear effects may become important. This is just the case for the kilometric radiation in its generation region (see Chapter 3). In the ULF and VLF ranges electromagnetic waves (naturally emitted or artificially injected) may also reach amplitudes which are sufficiently large to trap the particles and completely modify the physics of wave-particle interactions, opening the door to active modification of the magnetospheric environment. All this proves that the study of natural waves is far from being purely academic.

* *The lower value has been obtained by assuming a particle flux of $10^9$ electrons $cm^{-2}.s^{-1}$, an average energy of 10 keV and a precipitating area of (100 x 10000) $km^2$*

** *referenced to in Chapter 3*

The lectures are divided into 6 chapters :

1. Long period pulsations (< 0.1 Hz)
2. ULF waves (∿ 0.1 - 10 Hz)
3. VLF waves ( including kilometric radiation)
4. Electrostatic waves
5. Detectors
6. Analysing techniques

In an Appendix, the general relationships which exist between wave amplification and particle diffusion will be briefly discussed.



## CHAPTER I. LONG PERIOD PULSATIONS

Contrary to the other emissions which are more or less localized at least in their source region, the long period pulsations of the magnetic and electric fields ($T \gtrsim 10$-$20$ s) interest very large volumes, if not the whole, of the magnetosphere. Consequently, the physics which they involve is different from the localized microphysics which other electromagnetic or electrostatic emissions involve. The experimental techniques which are used for they study are also different : chains of magnetometers, bi- or multi-static radars, sets of spacecraft are tools which are necessary for understanding the spatial characteristics of these emissions.

Long period pulsations will be the subject of more detailed lectures by A.D.M. Walker. However it is useful to briefly review their main properties, the kind of physics which is involved in their propagation and generation and their principal consequences on the dynamics of magnetospheric particles.

### I.1. Basic ideas. Orders of magnitude

Magnetic field lines immersed within a plasma may oscillate at frequencies much lower than the ion gyrofrequency. The dispersion equation of these oscillations can be established by using the magnetohydrodynamic (MHD) theory* with suitable boundary conditions. In the case of the Earth's magnetic field lines, the existence of a highly conducting ground imposes that nodes exist there in the wave notion and in the electric field**. Standing waves are therefore to be expected. The field lines resonate, their resonance frequency being

* *usually by assuming an infinite parallel conductivity and by neglecting magnetic viscosity.*

** *The existence of an also conducting ionosphere with anisotropic properties and of a non conducting space between the ionosphere and the ground somewhat modifies this simple picture (see section I.3).*

given by :

$$T = 2 \int_S^N \frac{ds}{V_a} = \frac{2\ell}{\langle V_a \rangle} \qquad (2)$$

where the integral is taken along the field line of length $\ell$ between the two conjugate points on the ground, where $V_a = (B^2/\mu_o n m_i)^{1/2}$ is the Alfven velocity and $\langle V_a \rangle$ its average value, almost equal to the equatorial one *.

At L = 4 for instance, B ∿ 500 nT, n ∿ 100 $cm^{-3}$, $\ell$ ∿ 50000 km, so that $V_a$ ∿ 1000 $km.s^{-1}$ and T ∿ 100 s. This frequency lies in the Pc-4 frequency range (see Table 1). By assuming realistic models for the cold plasma density distribution along the field lines and radially across them, is is possible to compute the resonant frequencies for different values of L. On Figure 2, the results of such computations are given in a schematic form (Saito et al., 1976). One sees that a given period may correspond to 1 or 3 magnetic shells and that a given shell, in the vicinity of the plasmapause, may resonate at 2 much different frequencies, depending on its plasma content. The situation quoted $K_p$ = 2 corresponds to an inflated plasmapause, as compared with the situation quoted $K_p$ = 4. It may also be considered as representing the day situation (by opposition to the night one), since the plasma density at a given L value is larger on the day side than on the night side. This explains why a given frequency corresponds to a shell with a higher L-value during the day than during the night (see Figure 7)**.

* *A dipolar magnetic field is usually assumed. However in a recent publication Singer et al. (1981) claim to have computed better values for the pulsation period as a function of latitude and local time by introducing a more realistic model for the Earth's magnetic field. But their model is based upon unrealistic values of the cold plasma density (n=1cm$^{-3}$ at L=6.6 and constant along the whole field line). Moreover this model does not contain any local time variation of this density. Knowing that the plasma density may vary by a factor greater than 100 at the geostationary orbit whereas field intensity varies at most by 50%, it is clear that their conclusions are meaning less.*

** *It has been noted that, for a plasma density varying like $L^{-8}$, the period of oscillation is approximately independent of L. More field lines can resonate with the same frequency (Cavacinti et al., 1973).*



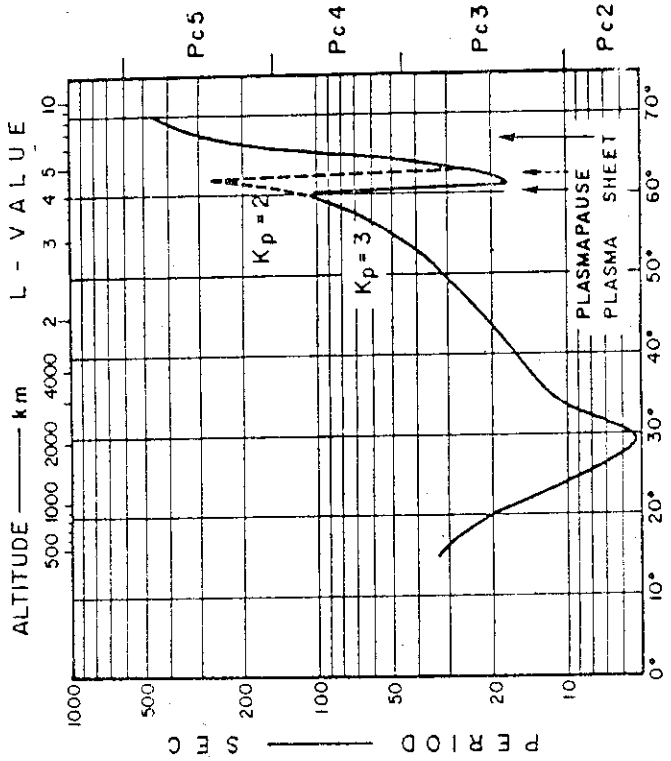


**Fig. 2**. Fundamental period T of the torsional oscillation of individual geomagnetic field lines. The magnetic field is represented by the dipole and field lines are labeled by the geomagnetic latitude of their intersection with the earth (see bottom) or by their equatorial crossing distance (see top). Period ranges of pc waves are indicated to the right of the figure. (Saito, 1976) and Nishida, Geomagnetic Diagnosis of the Magnetosphere, Springer-Verlag, 1978.

Simultaneous measurements of Pc-5 pulsations at different latitudes have confirmed these predictions, on a statistical basis : when averaged over many events, the latitude for which the signal has its maximum intensity is an increasing function of the period. But for each individual event, the frequency is independent of the latitude (Samson and Rostoker, 1972). Consequently whereas the concept of field line resonance can explain the passive properties of the medium (among all field lines excited by the same frequency, only those which resonate produce a large amplitude wave), there must be an independent excitation mechanism able to generate different frequencies for different events. This mechanism is likely to be oscillations of the magnetopause induced by the Kelvin-Helmoltz instability (see next Section), although wave-particule interactions have been also invoked (Section 1.5).

Magnetic field line resonance also implies the concept of mode parity (odd or even). In an axisymmetric model of the magnetosphere, one can also introduce the wave polarization by considering toroidal and poloidal modes. In the toroidal mode (also refered to as the transverse*, torsional, shear or Alfven mode), the total length of the field line does not vary. In the poloidal mode (also refered to as the compressional* or fast mode) the plasma displacement is radial and, for the odd modes, the length of the field line is oscillatory. These two concepts are explicited in Figures 3 and 4 (Southwood, 1981 ; Knox and Allan, 1981). Note that even in axisymmetric fields, the two polarization modes are coupled** and an analytical solution of the corresponding differential equations has not yet been found.

* *Note that "transverse" means that the azimuthal component of $\underline{b}$ ($b_\phi$) is different from zero and that "compressional" is not restricted to waves with a magnetic field $\underline{b} \parallel \underline{B}_o$, but to waves with $b_\phi = 0$.*

** *except for infinite azimuthal wave number, i.e. for the inphase oscillation of a whole magnetic shell (cavity resonance).*



Southwood, in "ULF pulsations in the Magnetosphere", D. Reidel, 1981

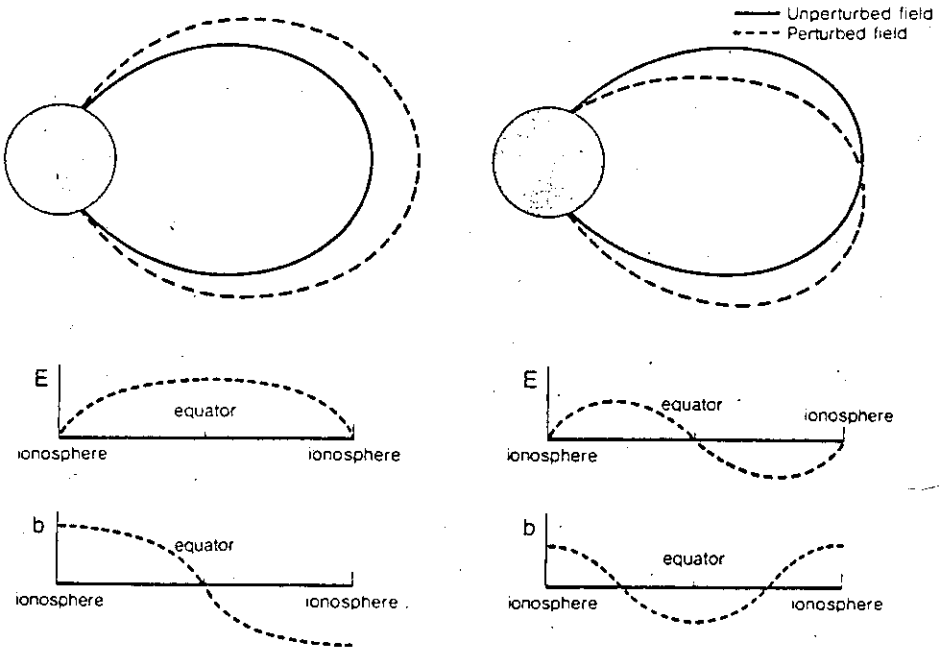


a) ODD MODE (fundamental) b) EVEN MODE (second harmonic)

STANDING OSCILLATIONS IN A DIPOLE FIELD

Fig.3. (a) Schematic of field line displacement (top), electric field amplitude along the background field (middle), and magnetic amplitude (bottom) in an odd mode fundamental standing Alfvén wave. (b) As for (a) for the lowest frequency even mode (second harmonic).

Knox @ Allan, in "ULF Pulsations in the Magnetosphere", D. Reidel, 1981




Fig. 4. Axisymmetric toroidal and poloidal modes.



Finally the ionosphere (with its anisotropic properties) and the neutral atmosphere below (with its non-conducting characteristics) play a role on the boundary conditions and therefore on the magnetospheric mode itself as well as on the wave characteristics as observed on the ground (see Section 1.3).

## 2. HM wave propagation through the magnetosphere

Theories of hydromagnetic (HM) wave excitation and propagation may be found in books or reviews (i.e. Dungey, 1963, 1968 ; Jacobs, 1970 ; Hasegawa and Chen, 1974 ; Nishida, 1978 ; Lanzerotti and Southwood, 1979). An important theoretical progress has been made when Chen and Hasegawa (1974) developed the theory of the coupling between a surface wave generated at the magnetopause and the shear Alfven wave propagating inwards. The variations as a function of latitude and local time of the wave amplitude and of the polarization which were predicted by the theory agreed well with the observations.

In Chapter 5 of his book, Nishida (1978) gave a simple demonstration of the approximate equations governing this propagation. For sake of simplicity all the field lines were assumed to be straight and to have the same length, $\ell$ in the unperturbed state. The field direction is taken as the z axis. The medium is assumed to be inhomogeneous in the x direction which is radially outward and the y axis is eastward. The perturbation fields are expressed as

$$\left.\begin{aligned} \underline{E} &= \left\{ E_x(x),\ E_y(x),\ 0 \right\} \exp\left[ i(\lambda y + kz - \omega t) \right] \\ \underline{b} &= \left\{ b_x(x),\ b_y(x),\ b_z(x) \right\} \exp\left[ i(\lambda y + kz - \omega t) \right] \end{aligned}\right\} \quad (3)$$

where the angular frequency $\omega$ and the original wave vector are specified by the source wave. The wavelength parallel to the magnetic field $\underline{B}\ \{0,0,B\}$ is equal to, or is an integral fraction of, $2\ell$. For waves of small amplitude and neglecting pressure gradient effects as compared to the Lorentz force, one gets, for the electric current perpendicular to $\underline{B}$ :

$$\underline{j}_\perp = \frac{\rho}{B^2} \frac{\partial \underline{E}_\perp}{\partial t} \qquad (4)$$

where $\rho$ is the plasma specific mass. By using $\nabla \times \underline{b} = \mu_0 \underline{j}$ and $\nabla \times \underline{E} = - \partial \underline{b} / \partial t$, one easily obtains

$$\left.\begin{aligned} (K^2 - k^2)\, E_x &= i\lambda \left( \frac{dE_y}{dx} - i\lambda E_x \right) \\ (K^2 - k^2)\, E_y &= \frac{d}{dx} \left( \frac{dE_y}{dx} - i\lambda E_x \right) \end{aligned}\right| \qquad (5)$$

where $K^2 = \omega^2 (\mu_0 \rho / B^2) \equiv \omega^2 / V_A^2$. Equations (5) lead to

$$\frac{d^2 E_y}{dx^2} - \frac{\lambda^2}{(K^2-k^2)(K^2-k^2-\lambda^2)} \cdot \frac{dK^2}{dx} \cdot \frac{dE_y}{dx} + (K^2-k^2-\lambda^2)\, E_y = 0 \qquad (6)$$

If the medium is homogeneous ($dK^2/dx = 0$) or if the wave vector is in the meridional plane ($\lambda = 0$), equation (6) reduces to the dispersion equation of a fast mode. In the presence of inhomogeneity and finite azimuthal wave number, the second term presents a singularity on the field line for which $K^2 = k^2$. This is the field line for which the resonant period $2\pi k/V_a$ is equal to the period $2\pi/\omega$ of the source wave. The singularity is logarithmic but by introducing a small imaginary part in the wave frequency, one gets a finite amplitude on the resonant field line. The variation of the wave amplitude as a function of -x is represented on Figure 5.

The polarization of the wave is easily shown, from equations (5), to be given by

$$\frac{b_y}{b_x} = - \frac{E_x}{E_y} = - \frac{i\lambda}{K^2-k^2-\lambda^2} \cdot \frac{1}{E_y} \cdot \frac{dE_y}{dx}$$



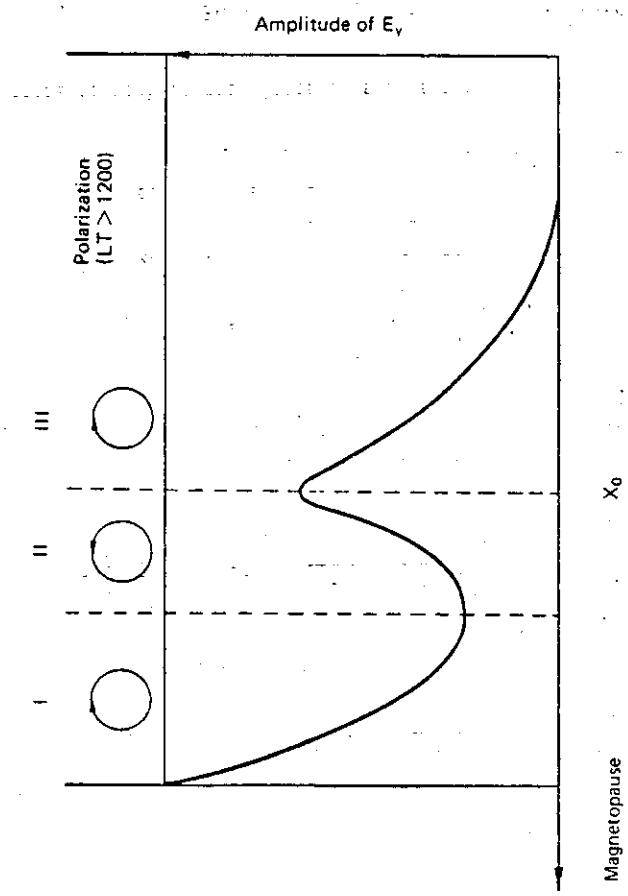


Fig. 5. Schematic representation of the distribution of amplitude and polarization of the hydromagnetic wave in the model magnetosphere. A monochromatic surface wave excited on the magnetopause is supposed as the source and $x_0$ denotes the resonant point (Southwood, 1974), Planet. Space Sci., 22, 483, and Nishida, Geomagnetic Diagnosis of the Magnetosphere, Springer-Verlag, 1978.

i.e. the polarization changes at each extremum of $E_y$. In particular, there is a polarization reversal at the resonance latitude. At the magnetopause boundary, $K^2 \ll \lambda^2$ so that $K^2-k^2-\lambda^2$ is always negative and the polarization sense is everywhere defined by the sign of $\lambda d(\text{Ln } E_y)/dx$. For eastward propagating waves ($\lambda > 0$) it has the sense represented on Figure 5. For westward propagating surface wave ($\lambda < 0$) the polarization is opposite.

It is worth noticing that the relationship which is thus established (without any reference to a specific excitation mechanism except that it is a surface wave of short azimuthal wavelength) between the sense of polarization and the direction of propagation is exactly the one which is compatible with an excitation of the Kelvin-Helmoltz instability by the solar wind blowing around the magnetopause (Figure 6) *.

These local time and latitude variations of the polarization are also exactly the ones which were observed, first at a high latitude by Nagata et al. (1963) for Pc-5 oscillations, second at different latitudes and for Pc 4-5 oscillations by Samson et al. (1971) by using the Canadian magnetometer chain. These last authors also showed that the polarization reversal occurred at the latitude for which the wave amplitude is maximum (Figure 7).

The azimutnal direction of the propagation also agrees with the theory : it changes from westward direction in the morning to an eastward direction in tne afternoon. This has been observed both on the ground, by using three stations situated at a geomagnetic latitude $\Lambda = 67.3°$ and separated in longitude by ~ 5° (Olson and

* *Note that if the magnetic moment of the Earth had its polarity reversed such a coincidence would not occur. Waves generated by the Kelvin-Helmoltz instability would not propagate deep into the magnetosphere. Inward diffusion of energetic particles would be drastically reduced and precipitation in the auroral zone should be enhanced.*



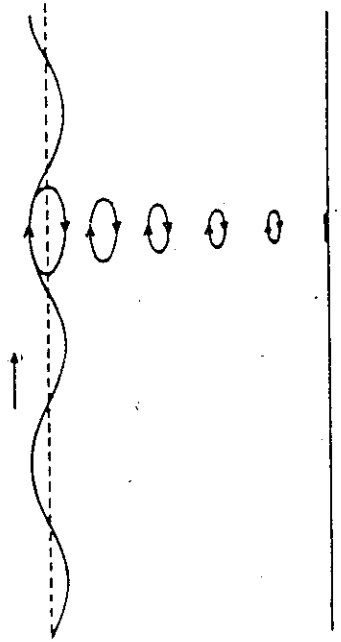

Jacobs, "Geomagnetic Micropulsations", Springer-Verlag, 1970

Fig. 6 a. Motion of fluid elements in a free surface wave

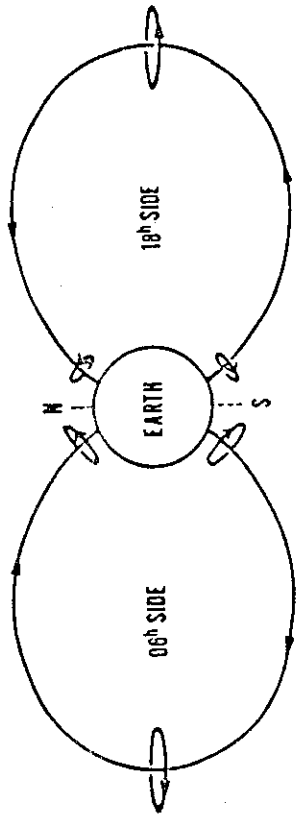


Fig. 6. b. Model showing the polarization of long period geomagnetic micropulsations (viewed from the sun). (After T. Nagata, S. Kokubun and T. Iijima)

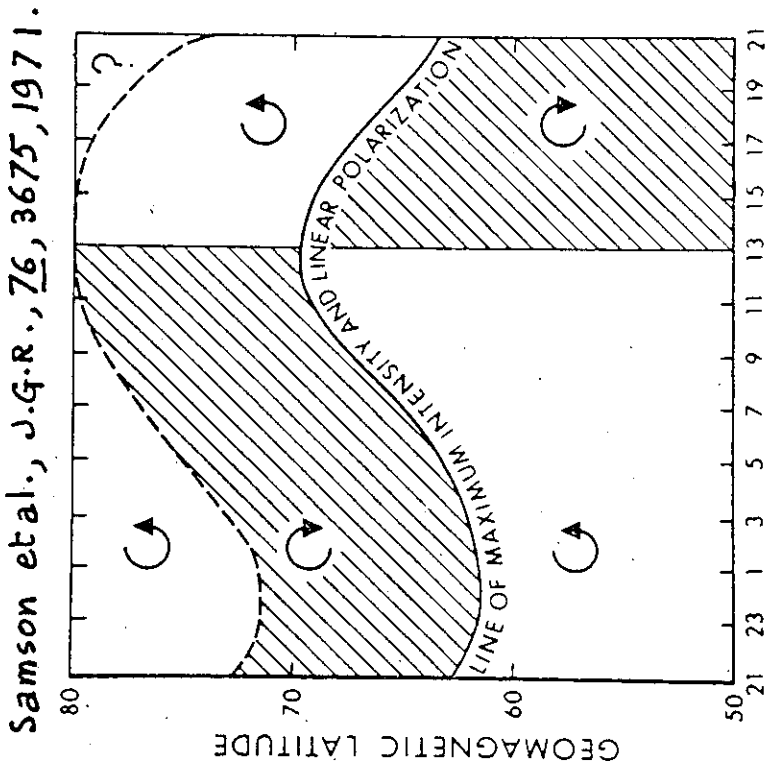


Fig. 7. The statistical diurnal variations of the polarization characteristics of quasi-monochromatic magnetic variations with frequency ~5 mHz. (Copyright by American Geophysical Union, 1971.)



Rostoker, 1978), and in space by using three geostationnary satellites separated by approximately the same longitude difference (Hughes et al., 1978). In the first experiment the azimuthal wave number was shown to vary with frequency :

$$m = (1.4 \pm 0.4)\ f + 0.26 \qquad (8)$$

where f is in mHz. The phase velocity at the ground is

$$v_{\phi g} = (2\pi R_e \cos\Lambda)\cdot(f/m) \approx 2\pi R_e \cos\Lambda / (1.4 \pm 0.4) \times 10^3 \qquad (9)$$

where $R_e$ is the Earth radius. Therefore the phase velocity is independent of frequency and it is of the order of 14 $km.s^{-1}$. The corresponding value at the magnetopause boundary is $v_{\phi b} = (15/\cos\Lambda)v_{\phi g}$ if one assumes that the magnetopause distance to the center of the Earth is 15 $R_e$. This leads to phase velocities at the boundary of the order of 400 $km.s^{-1}$ which is the order of magnitude of the solar wind speed. In the second experiment, wave numbers of the same order of magnitude ($m \sim -5$ to $-10$ for $f \sim 6$ mHz) were observed in the morning sector (Figure 8).

However, not all the experimental results agree with the theory, especially for long period pulsations that are observed at lower latitudes ($\sim 45°$). For instance, the polarization reversal is not always observed at the latitude where the signal amplitude is maximum. The observed frequencies may also be smaller than the ones which are predicted by the theory (equation (2) or equivalent expressions) when measured values of the plasma density are introduced (Stuart and Lanzerotti, 1982).

## 1.3. The role of the ionosphere

Because of its anisotropic properties and of its layered structure, the ionosphere modifies the wave structure. This effect will be described in more detail by A.D.M. Walker in his lectures.

Hughes, McPherron & Barfield
J.G.R., 83, 1109, 1978.
Also Hughes, in "ULF Pulsations
in the Magnetosphere", D. Reidel, 1981,
pp. 41-58.

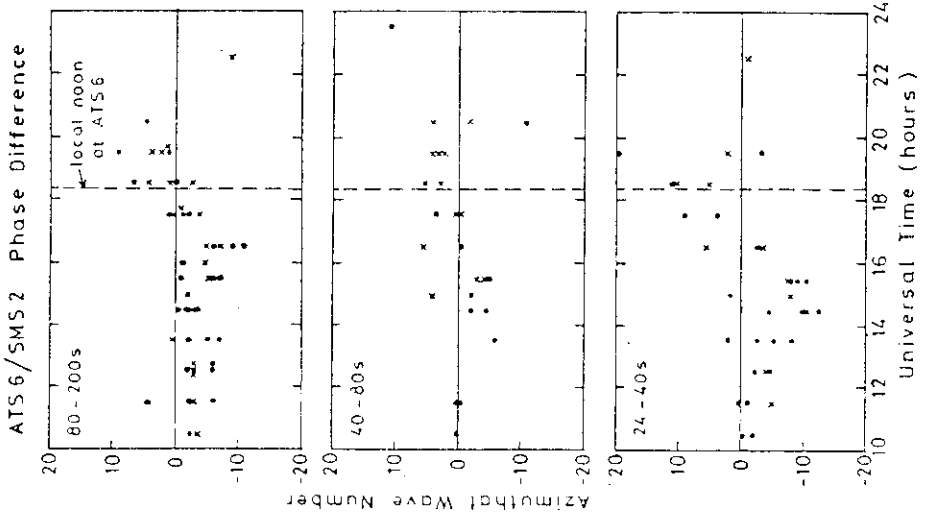


Fig. 8. The azimuthal wave number, *m*, obtained for waves which were coherent between SMS 2 and ATS 6, plotted as a function of universal time. Dots and crosses refer to values obtained from azimuthal and radial components respectively.



Its main consequence is the ∿ 90° rotation of the wave magnetic field between the top of the ionosphere and the ground. It is sufficiently important to be briefly described here.

A simple argument for explaining this rotation has been given by Hasegawa and Lanzerotti (1978). The toroidal mode, in the magnetosphere, is such that $b_z = 0$. The magnetic field being divergence-free, one has

$$\left( \frac{\partial b_x}{\partial x} + \frac{\partial b_y}{\partial y} \right)_m = 0 \qquad (10)$$

At the ground, there is no parallel current. Therefore $(\underline{\nabla} \times \underline{b})_z = 0$, which leads to

$$\left( \frac{\partial b_y}{\partial x} - \frac{\partial b_x}{\partial y} \right)_g = 0 \qquad (11)$$

from which one deduces the relations

$$\left.\begin{aligned} b_{xg} &= c\, b_{ym} \\ b_{yg} &= -c\, b_{xm} \end{aligned}\right\} \qquad (12)$$

where c is a constant and which show that there is a 90° rotation of the magnetic component of the wave, the electric field of the wave being not modified.

However this argument is uncomplete : an identical one could give as well the following equivalence

$$\left.\begin{aligned} b_{xg} &= -c\, b_{ym} \\ b_{yg} &= c\, b_{xm} \end{aligned}\right\} \qquad (13)$$

xhich also corresponds to a 90° rotation but in the opposite direction.

It will be shown below that the correct transformation for the northern hemisphere is given by equations (12) and not by equations (13), when assuming that x is directed northward and y is directed eastward. In the northern hemisphere the ground magnetic field (when looking toward the ground) is rotated in the counterclockwise direction with respect to the field prevailing at the top of the ionosphere. The opposite is true in the southern hemisphere.

The physical reason for this rotation is the following. The Pedersen current induced in the conducting ionosphere by the electric field of the wave produces on the ground a magnetic field $\underline{b}_{gP}$ which almost cancels the original one ($\underline{b}_m$). But the Hall current produces on the ground a magnetic field $\underline{b}_{gH}$ which is in the same direction as the original electric field $\underline{E}_m$ (Figure 9). Because the wave is propagating towards the ground, ones goes from $\underline{b}_m$ to $\underline{E}_m$ (and therefore to $\underline{b}_g$) in a counterclockwise direction (as seen from above). A simplified transformation formula (Nishida, 1978)* is

$$\left.\begin{aligned} b_{xg} &= 2\,\frac{\Sigma_H}{\Sigma_P}\cdot\exp\left[-|m|\,d\right]\cdot b_{ym} \\ b_{yg} &= 0 \end{aligned}\right| \qquad (14)$$

where m is the wave number of the perturbation in the horizontal direction and d the distance between the ground and the ionospheric conducting layer ($d \sim 120$ km). $\Sigma_H$ and $\Sigma_P$ are the height-integrated Hall and Pedersen conductivities. Because of the $\exp[-|m|d]$ factor, the ionospheric attenuation is larger for waves having shorter horizontal wavelengths.

A more complete study of this effect has been made by Hughes and Southwood (1976a). Figure 10 gives an example of their results for $m_x = 4 \times 10^{-2}$ km$^{-1}$, $m_y = 0$ and $\omega = 0.1$ s$^{-1}$. In a following paper (Hughes and Southwood, 1976b) these authors have combined this effect

* *see also the review by Walker and Greenwald, 1981*



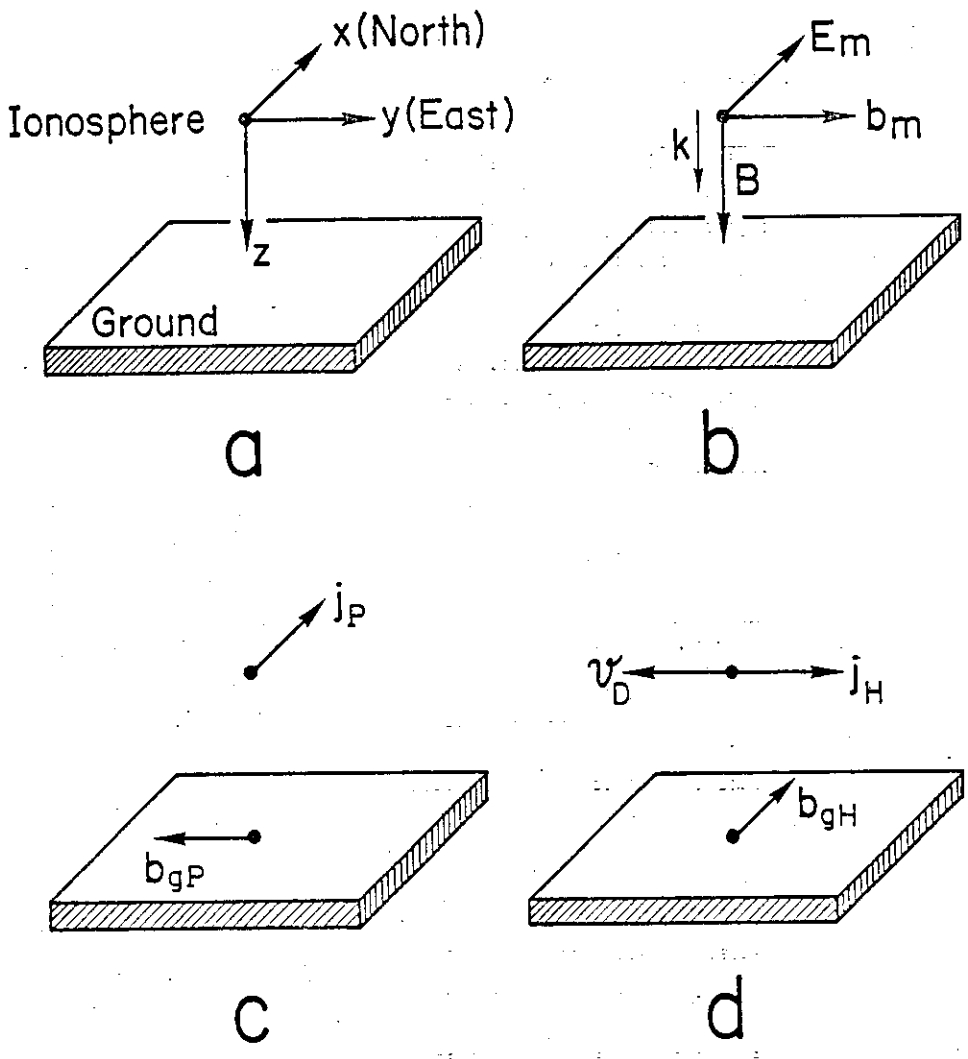


Fig.9. Ground rotation of the magnetic field of a magnetospheric Alfven wave impinguing upon the ionosphere. a/ Coordinate system. This system is the projection, in the northern hemisphere, along the magnetic field lines of the system used for the study of magnetospheric wave propagation (section 1.2). It differs from the one used by Hugues and Southwood (Fiures 10 and 11). b/ Electric and magnetic fields of a toroidal wave at the top of the ionosphere. c/ Pedersen current and associated magnetic field. d/ Hall current and associated magnetic field (ions being at rest, $\underline{j}_H$ is opposite to $\underline{V}_d = \underline{E} \times \underline{B}/B^2$).

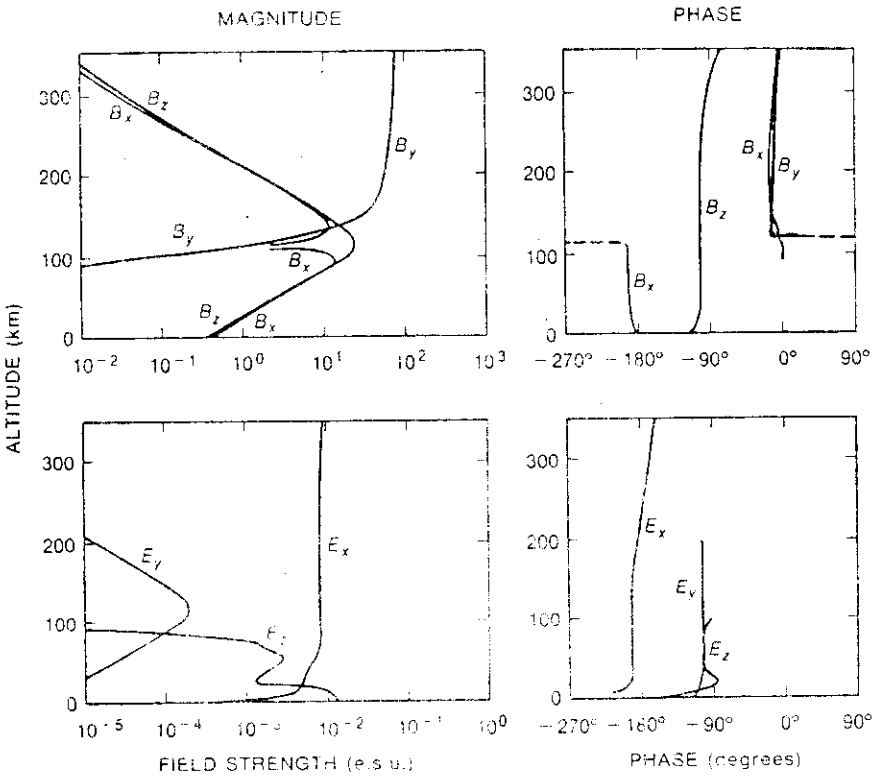


Fig. 10. Vertical profiles of the magnetic and the electric perturbation fields in a model calculation using the daytime, sunspot maximum ionosphere model (Hughes and Southwood, 1976a) and Nishida, 1978.



with the results of the magnetospheric propagation theory which imposes the x variation of the magnetospheric wave field (Figure 11, where the origin of the latitudinal distance corresponds to the resonance field line and where a small longitudinal variation has been superimposed : $m_y = 10^{-3}$ km$^{-1}$. The angular frequency is the same as before : $\omega = 0.1$ s$^{-1}$). Improvement of the theory has been brought in later studies (see Knox and Allan, 1981 for a review).

The experimental observation of such an effect has been made by comparing the magnetic component of Pc 4-5 pulsations detected at the ground with data obtained on the ionospheric field by using remote sensing techniques. These techniques are of two kinds : the incoherent scatter radar, like the one operating in France at Saint-Santin (Lathuillière et al., 1981) or the multi-static coherent radar system operating in the Scandinavian auroral zone (Walker et al., 1979)*.

## 1.4. Experimental results

In the previous section we have just presented the basic experimental facts which confirmed (or which have initiated) theoretical works. In this Section, we will present more experimental data on the characteristics of these long period pulsations or on their relationships with other geophysical phenomena. These characteristics or relationships are far from being all well established and more experimental (and reliable) works have to be achieved in this field.

### Occurrence

Figure 12 shows the results of a study made by Kokubun (1981) on the occurrence of Pc 4-5 pulsations detected simultaneously on the ground and on board ATS-6. These pulsations occur preferentially in the morning sector (with a secondary peak around dusk), during moderately active periods. The figure also shows that the morning

* *see also the review by Walker and Greenwald, 1981*

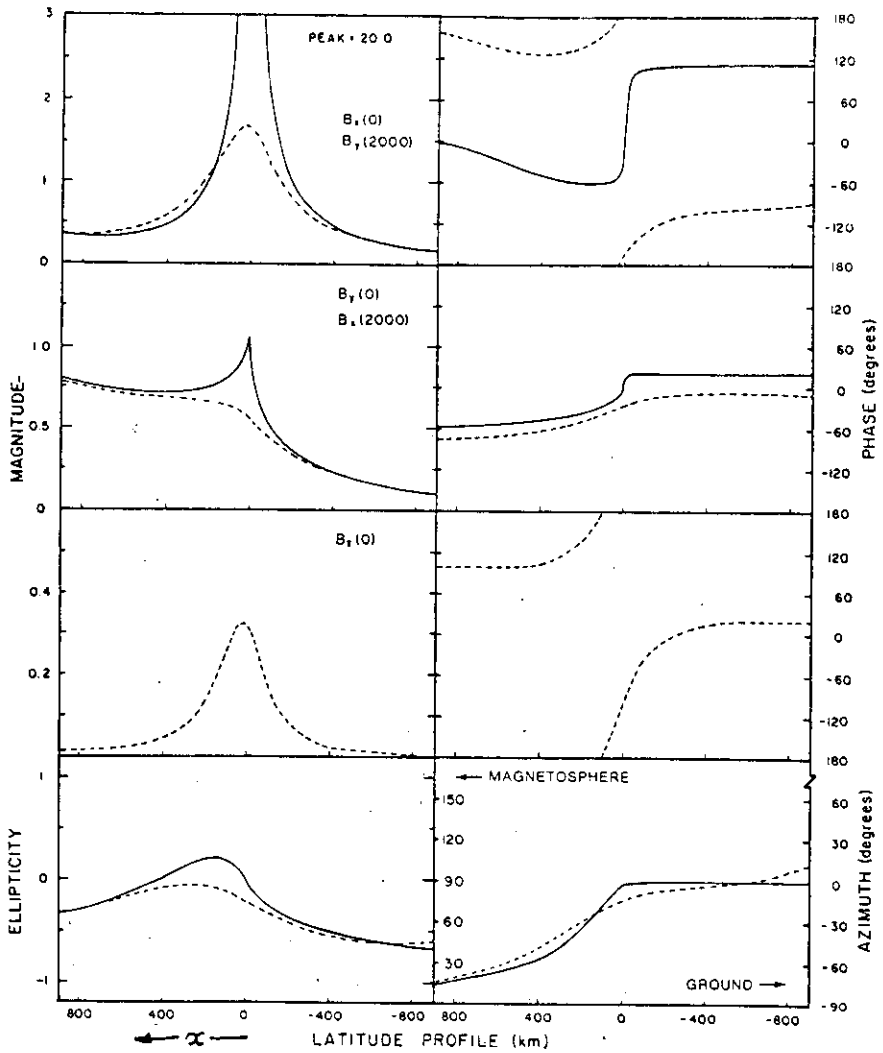


Fig. 11 . Calculated latitude profiles of the magnetic field components and polarization characteristics at the ground level (------) and at the altitude of 2000 km (———). The ionosphere is assumed to be at the daytime sunspot minimum condition (Hughes and Southwood, 1976b). Only Alfven-mode wave is assumed to be present above the ionosphere. Azimuth is measured clockwise from the north (x being northward and y westward).



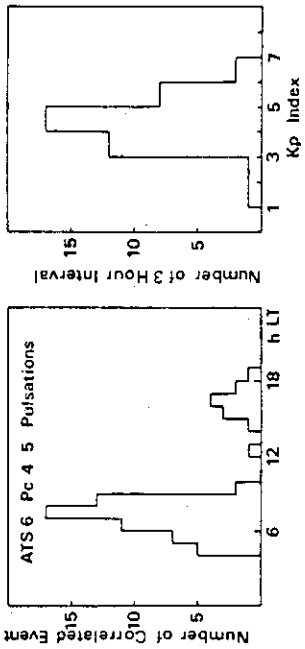


Local time distribution and $K_p$ dependence of occurrence of ground-correlated Pc 4-5 waves at ATS 6.

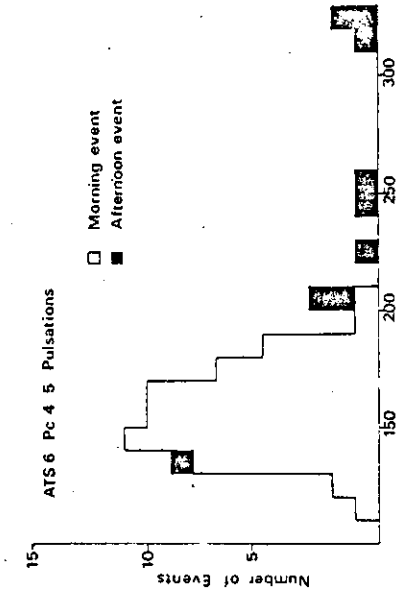


Period distribution of ground-correlated Pc 4-5 waves observed at ATS 6.

Figure 12. From Kokubun, 1981

oscillations have more stable periods (with a peak value of the order of 150s). However, other studies made with the same spacecraft, when it was situated at a different longitude, have provided different results, the maximum of occurrence being situated around noon and the average period being of the order of 60s (see Kokubun's Figure 11).

Intensity

Between 0.2 and 50 mHz, ATS-6 data and data from other spacecraft or from the ground have been used for establishing the average power spectra of pulsations in different magnetospheric regions (Arthur et al., 1978). In Figure 13 where these results are reported the symbols represent, IMF : interplanetary medium, MSH : magnetosheath, NM : near the magnetopause, SYN : synchronous orbit, GRD : ground. The slope of log PSD/log f where PSD is the power spectral density varies between - 1.44 (MSH) and - 2.23 (GRD). These average values have been obtained without making any selection with respect to local time, position or magnetic activity. As far as the last parameter is concerned an increase of almost 2 orders of magnitude of the PSD is observed when the magnetic activity increases from quiet conditions ($\Sigma K_p = 0$) to moderately disturbed ones ($\Sigma K_p = 24$).

Mode structure

It is important to know the mode number of the standing wave which is observed. Otherwise it is impossible to uniquely relate the plasma parameters (the density for instance) to the quantity which is measured (the period). Dynamic spectral analyses* of the pulsations detected on board ATS-6 have shown that many modes are present simultaneously (Takahashi and Mc Pherron, 1982). Peaks in the PSD have been observed at the harmonics (n = 2, 3, 4, ...) of a same frequency, the fundamental (n = 1) being almost always absent. The absence of the fundamental is natural when the observation of an Alfven wave is made on its magnetic component when the spacecraft is in the vicinity of

* *known as 'sonagrams' (see Chapter 6)*



Arthur, McPherron, Lanzerotti @ Webb, J.G.R., 83, 3859, 1978

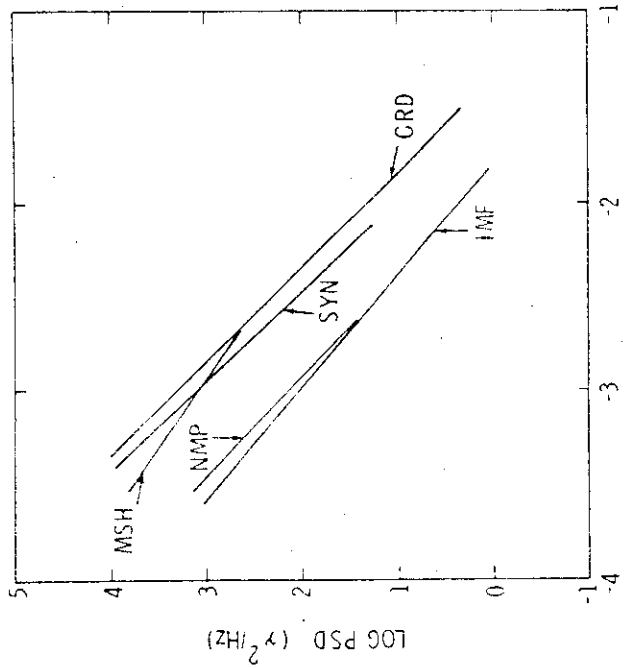


Fig. 13. Average power spectra for the five regions. The symbols are explained and the slopes are given in Table 2.

the equator (see Figure 3). The relative amplitudes of the harmonics in this region can be computed if one has a model of the plasma density distribution along the field line and if their relative amplitudes are known at another point. An example of the results of such a computation is shown on Figure 14 which was obtained by assuming a plasma density distribution of the form

$$n = n_o \, (r_o / r)^{-4} \qquad (15)$$

where r is the geocentric distance along the field line and $r_o$ its value at the apex. The amplitudes are normalized to their ground values. Examination of Figure 14 shows that the relative amplitudes of the different harmonics vary with the latitude of observation (the latitude of ATS-6 varied because this spacecraft was moved in longitude). Note however that one cannot use these curves to precisely predict the observed amplitude ratios, which much depend on their assumed values at the ground level.* The order of the lowest harmonic being known (n = 2) it is possible to evaluate $n_o$. For some events Takahashi and Mc Pherron (1982) found values increasing steadily from $\sim 3$ cm$^{-3}$ at 08.00 LT to $\sim 8$ cm$^{-3}$ at 13.00. These values (and their trend) are in good agreement with those deduced from the active resonance sounder experiment on board GEOS-2 (Higel and Wu Lei, 1982).

Another method can be used in space for evaluating the mode parity. It consists in measuring the phase difference between the magnetic field vector and either the plasma velocity (Kokubun et al., 1977) or the electric field (Singer et al., 1982). The phase lags which are expected for different mode parities between these quantities are represented on Figures 15 and 16. (In Figure 16, x is radially outward and y azimuthally eastward). By applying the first method to OGO 5 data, Kokubun et al. (1977) showed that most of the events

* *This is clear proof that more experimental studies are needed !*



Takahashi @ McPherron, J.G.R., 87, 1504, 1982

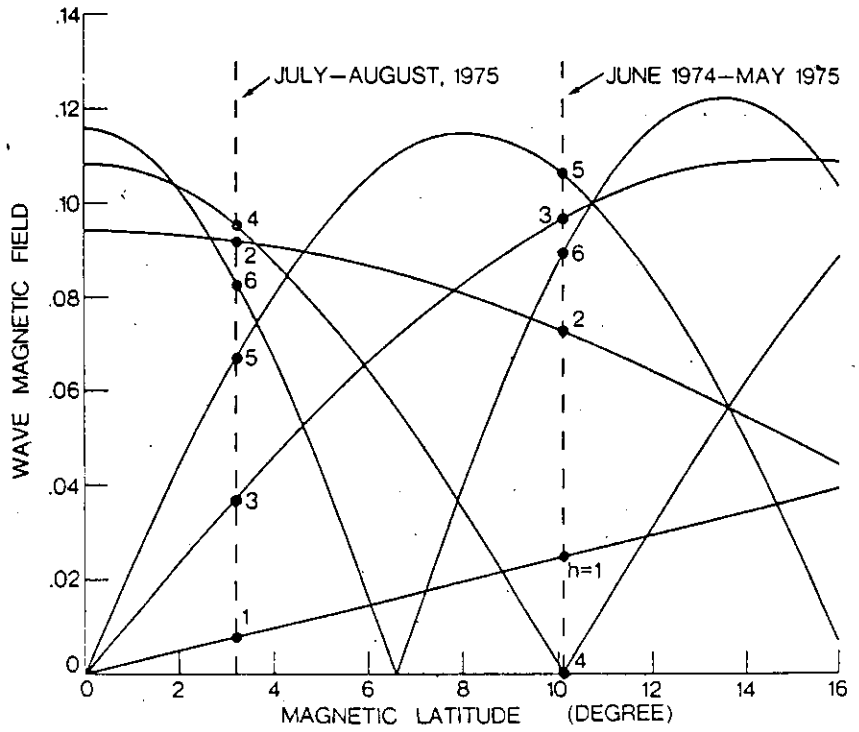


Fig.14 . Wave magnetic field of the toroidal mode waves. The amplitude is normalized by the value at the surface of the earth.

JGR, 82, 2774, 1977.

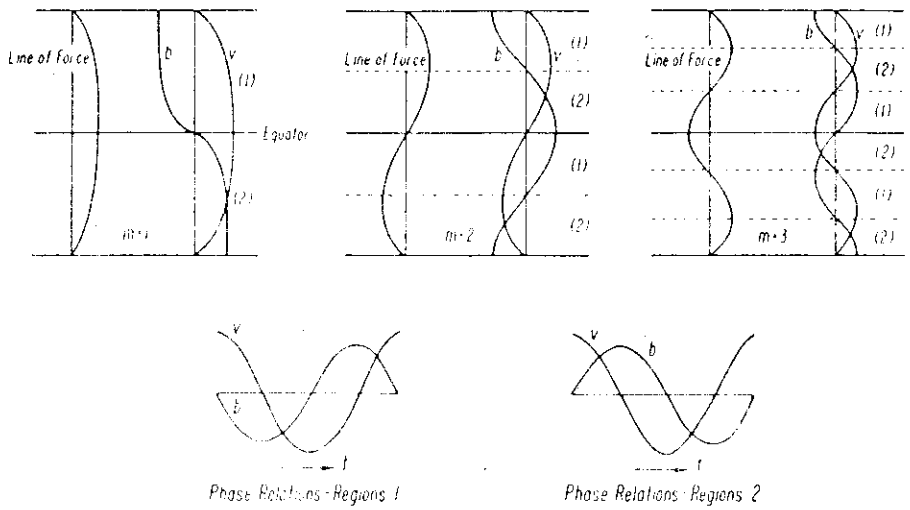


Fig. 15. (Top) Schematic representations of standing waves along a field line. The three lowest modes of a field line oscillation are represented with the curves indicating the maximum displacement of the field line from its equilibrium position (straight vertical line). For each mode the spatial variation of the magnetic perturbation b at the time of maximum field line displacement and of the plasma velocity v at the time of zero displacement are displayed schematically. The vertical axis represents zero perturbation. Along the field line, regions are labeled 1 and 2, depending on the phase relations between b and v. (Bottom) Velocity and field perturbations at a fixed point within regions of types 1 and 2 plotted as functions of time.



JGR, 87, 3519, 1982.

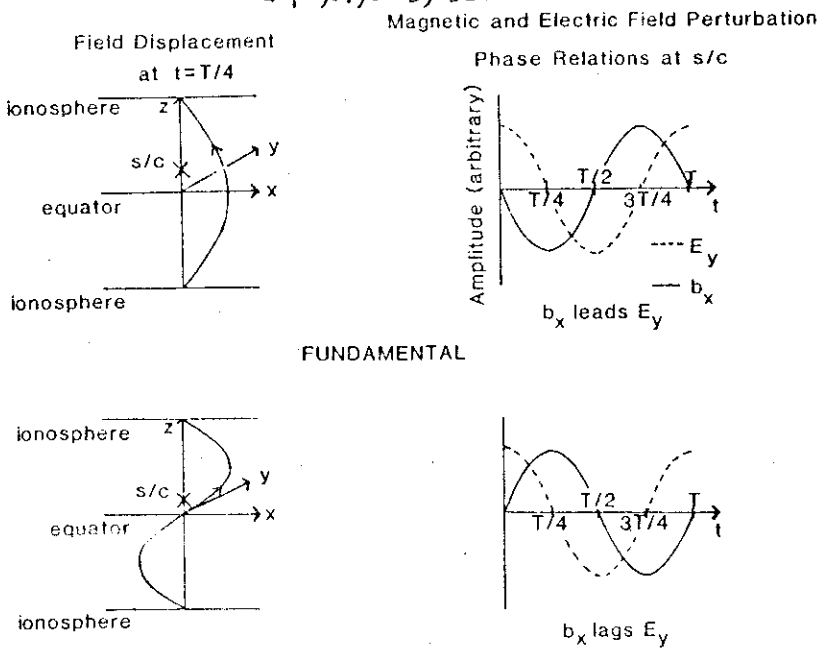


Fig. 16. Schematic illustrating the expected magnetic and electric field perturbation phase relations for the fundamental (odd mode) and second harmonic (even mode) oscillations. The left side of the figure shows the maximum excursion of the magnetic field line in the $x$-$z$ plane about its equilibrium position after one fourth wave cycle. The right side of the figure shows the magnetic and electric field perturbation as a function of time measured by a spacecraft from a position slightly above the magnetic equator.

corresponded to odd mode standing waves (n = 1, 3, ...). On the contrary Singer et al. (1982), by applying the second method to ISEE 1 and 2 data found that most of their events were even mode standing waves (n = 2)*.

Spatial extension

In their already quoted work Hughes et al. (1978) found that the longitudinal extension of the wave at the geosynchronous orbit was ∿ 20° and that the oscillations were in phase over a limited range of radial distances (0.2 - 0.5 $R_e$), which implies a strong selectivity of the excited magnetic shells, as expected. The radial extension of Pc 4 waves was also studied by Singer et al. (1982) with ISEE 1 and 2. They found it to lie between 0.2 and 1.6 $R_e$.

Polarization reversal

Most of the original works dealing with the local time or latitudinal variations of the Pc 4-5 polarization were done by using magnetometer data (see Section 1.2). Recently the STARE** electric field data have been used to show the polarization reversal of the waves as a function of latitude (Villain, 1982). Figure 17 gives an example of the results thus obtained for the morning hours. The observed polarization agrees with the predictions of the Kelvin-Helmotz instability theory. The polarization reversal clearly coincide with the maximum amplitude (dashed line).

Ionospheric effects

Besides of the comparison between the ionospheric E field and the ground b field (see the previous Section), the b rotation induced by the presence of the ionosphere has recently been put in evidence by an original method based upon the change of the magnetic field length for poloidal oscillations (Andrews et al., 1981).

* *This is a clear proof that more experimental studies are needed !*

** *Scandinavian Twin Auroral Radar Experiment.*



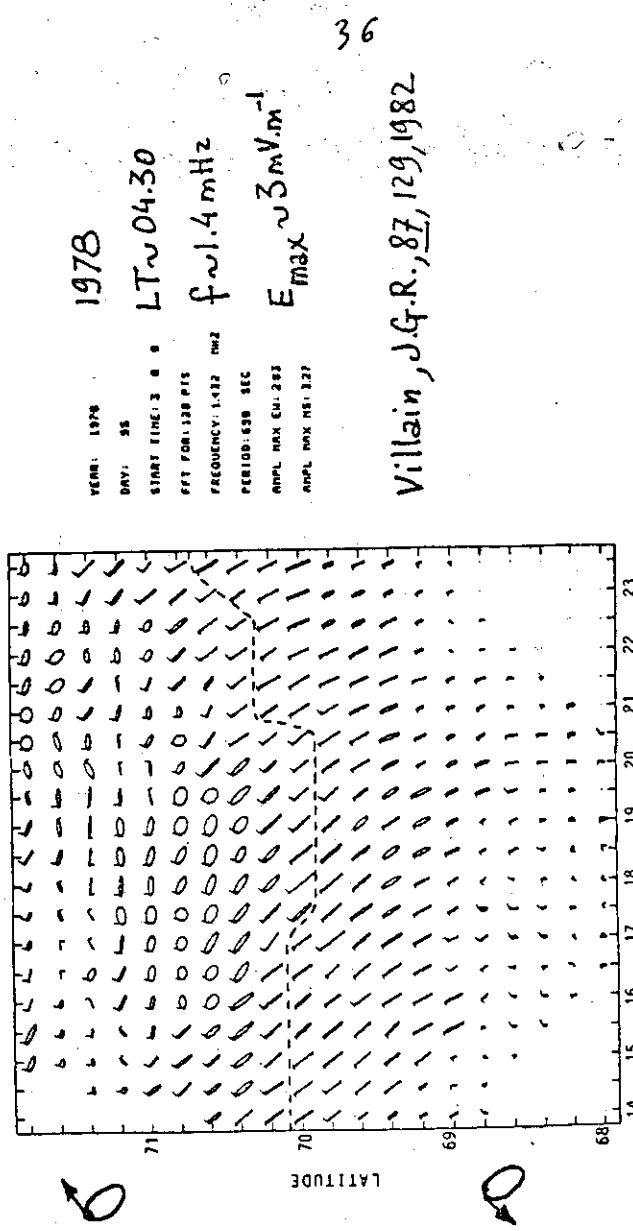


Fig. 17. Two-dimensional polarization map obtained for a 698 s period for event 1. For each geographic point of the STARE field of view the polarization ellipse of the electric field is drawn as described in Figure 4.

Powerful VLF transmitters emit signals which can propagate in the whistler mode* within magnetospheric ducts and which are received at the conjugate point. Often these signals are subject to small Doppler shifts ($\Delta f < 1$ Hz) due to the variation of the duct length. On some occasions these Doppler shifts oscillate at ultra low frequencies in conjunction with long period pulsations of the same frequency.

Toroidal oscillations would not affect the phase path length but poloidal ones do. If the field line is moved from its unperturbed position (corresponding to a phase path length $\phi_o$) to another position for which the phase path length becomes $\phi$, the change of the orientation of the field line produces a variation of the horizontal component of the magnetic field, as shown on Figure 18 for the fundamental mode. One can write

$$\phi = \phi_o - k\, b_N \tag{16}$$

where k is a positive constant. Therefore

$$\Delta f \equiv - \dot{\phi} = k\, \dot{b}_N \tag{17}$$

If there were no rotation of the magnetic field between the top of the ionosphere and the ground, the H component measured on the ground would be equal to $b_N$, so that one would have

$$\Delta f = k\, \dot{H} \tag{18}$$

On the contrary, if there is an ionospheric effect, such as the one theoretically predicted (a 90° counterclockwise rotation in the Northern hemisphere), one will have

$$\Delta f = - k\, \dot{D} \tag{19}$$

Correlation techniques have been used which show that equation (19) is indeed verified (Figure 19).

* *See Chapter 3*



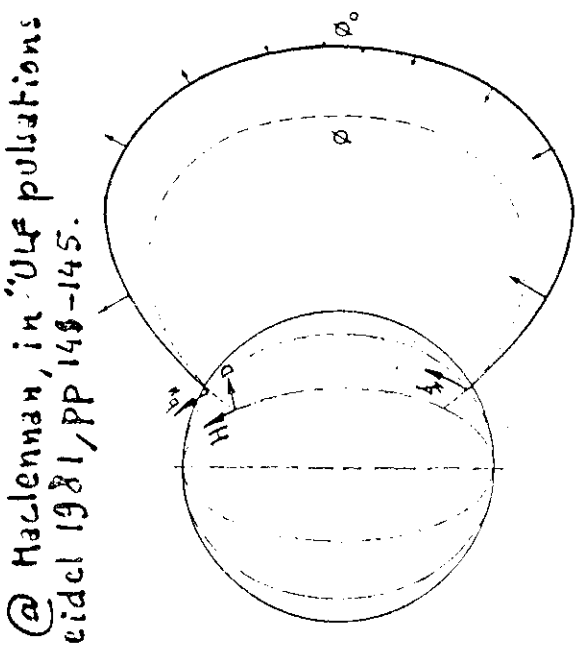


Fig. 18. Relation of VLF phase path to pulsation signals on the ground.

(Andrews, Lanzerotti @ Maclennan, in "ULF pulsations in the magnetosphere", D. Reidel 1981, PP 148-145.

M. K. ANDREWS, L. J. LANZEROTTI, and C. G. MACLENNAN
in "ULF Pulsations in the Magnetosphere", D. Reidel, 1981.

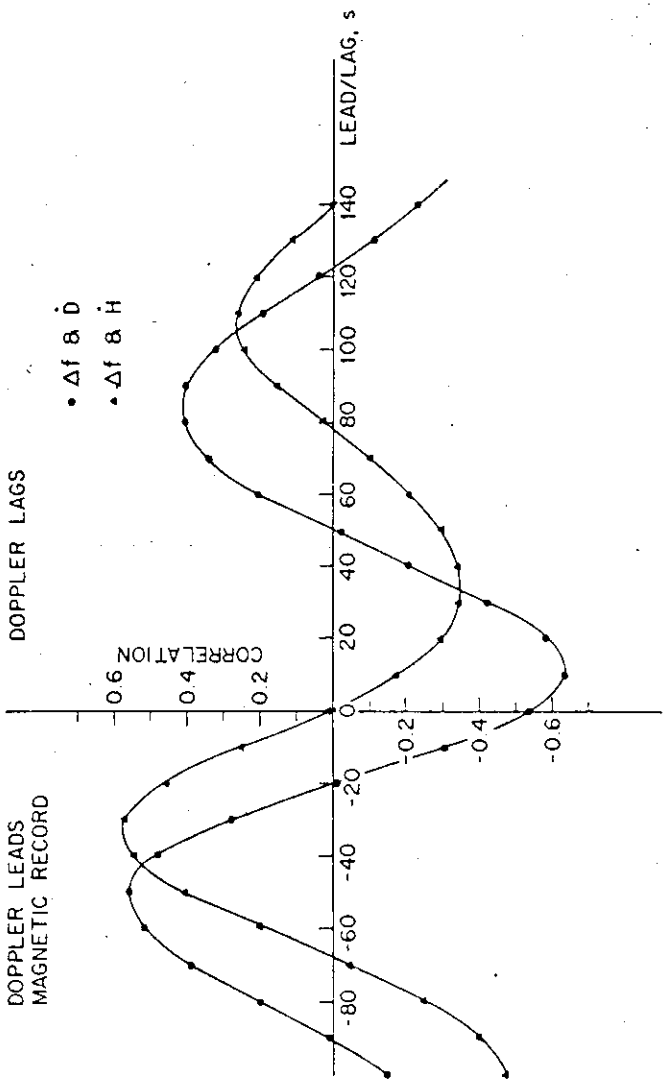


Fig. 19. Cross correlation of Siple whistler mode signals and magnetic data from Durham, hour 16, July 6, 1975.



Relationships with solar wind parameters

A lot of studies have been devoted to this subject. But the linkage between the various properties of geomagnetic pulsations and various parameters of the solar wind is rather loose. Correlations which were claimed to exist by some authors were demonstrated by others not to exist. The only correlations which seem presently to be well established concern :

- the pulsation occurrence with IMF orientation,
- the pulsation periods with IMF strength,
- the pulsation amplitudes with the solar wind velocity.

The two last correlations are illustrated on Figures 20 and 21. Students are referred to the review by Greenstadt et al. (1981) for a detailed discussion of this problem.

Associated particle fluctuations

That energetic particle fluxes* detected on board spacecraft could present oscillations at frequencies in the Pc 4-5 range is known since long (i.e. Laquey, 1973 ; Baxter and Laquey, 1973). Recent studies of phenomena observed on board excentric (i.e. Kokubun et al., 1979 ; Engelbretson and Cahill, 1981) or geostationary spacecraft (i.e. Hughes et al., 1979 ; Su et al., 1977, 1979, 1980 ; Kremser et al., 1981) have emphasized the association between these flux oscillations and hydromagnetic pulsations. One example of such wave-associated flux oscillations is given on Figure 22. The main conclusions which can be drawn from these observations are :

- the total particle density (ions + electrons) oscillates out of phase with the magnetic field intensity : the sum of the kinetic and magnetic energy densities remains more or less constant (Hughes et al., 1979 ; Kremser et al., 1981).

* *in the energy range from ∿ 1 keV to ∿ 200 keV, both protons and electrons.*

Gul'elmi et al. (1973)

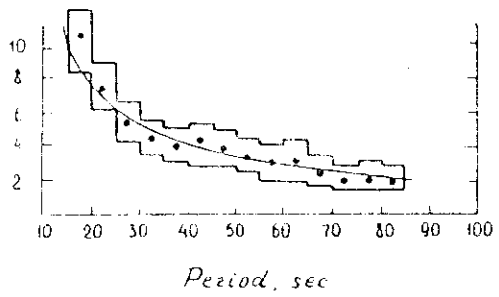


Greenstadt, McPherron @ Takahashi in "ULF Pulsations in the Magnetosphere", D. Reidel, 1981, pp 89-110.

41

Veró and Holló (1978)

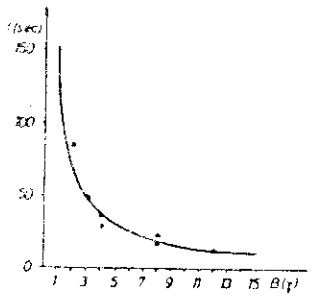


Fig. 20 Two versions of the observational results relating $B$ in the solar wind to the period $T$ of daytime pulsations. The curves are drawn from $T = 160/B$.

42

Fig 21 — Pc-4 amplitude and solar wind velocity

Greenstadt, Singer, Russel and Olson (1979)

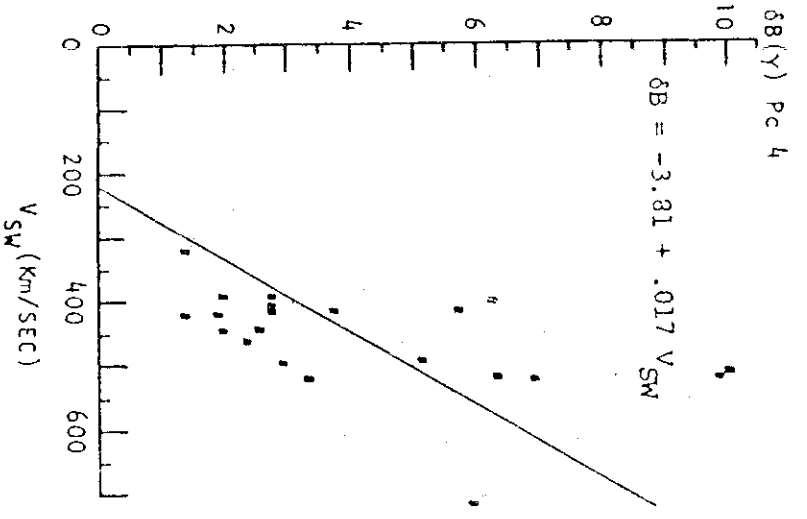

Kremser et al., J.G.R., 86, 3345, 1981.

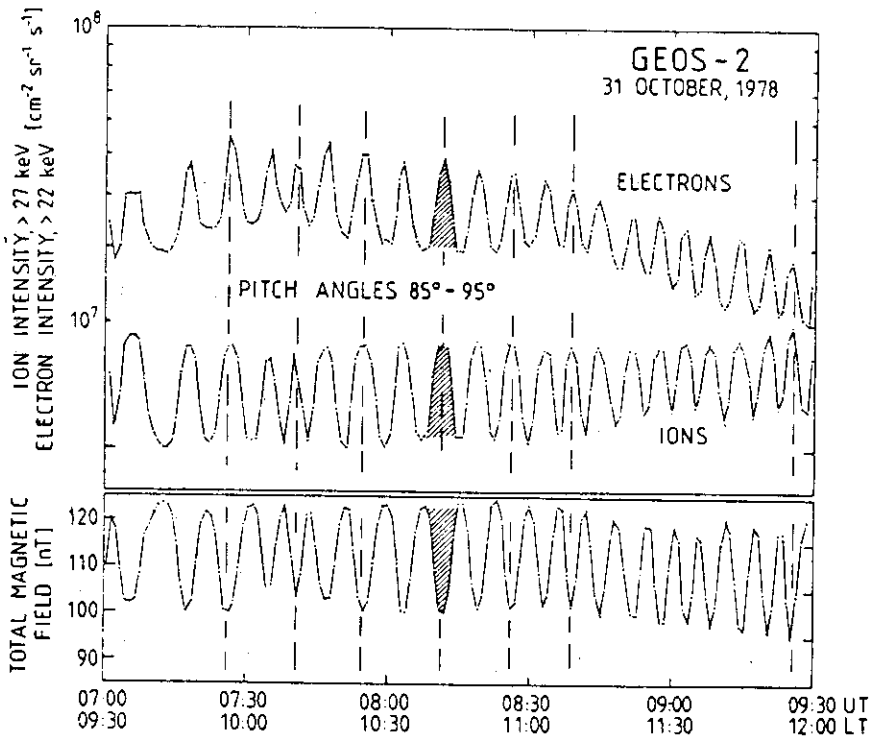


Fig. 22. Example of in-phase variations of the fluxes of electrons and ions. This is a part of an in-phase event that lasted 8 hours. The top part contains 60.6-s averages of the electron intensity (>22 keV) and the ion intensity (>27 keV) in the pitch angle range of 85°–95°. The bottom part represents the variation of the total magnetic induction at GEOS 2. The vertical dashed lines were drawn to facilitate the comparison of the relative phases. The hatched area indicates a period that is discussed in more detail in section D1 (see Figures 4–6).



- The ULF wave has always a compressional component ($b_{//}$), which may reach values as large as 30γ (Kremser et al., 1981).

- In the energy range ∿ 5 - 200 keV, the modulation is more easily seen on the protons than on the electrons. The proton modulation amplitude is larger at higher energies (Su et al., 1979, 1980 ; Kremser et al., 1981). The ratio $(J_{max} - J_{min}) / (J_{max} + J_{min})$ may reach values as high as ∿ 4 (Su et al., 1980).

- The modulation amplitude is also a function of the pitch angle (Su and al., 1980).

- The phase relationships between $J_e$ and $J_p$ depends on the local time, $J_e$ and $J_p$ being in phase in the morning and at noon, and out-of-phase at dusk. This effect is linked with the change of the shape of the electron pitch angle distribution from pancake to butterfly when going from the morning side to the late afternoon side (Kremser et al., 1981).

- The phase relationship between the proton flux and the wave amplitude is a function of the particle energy (Su et al., 1980).

These phenomena are so complex and they have such a large amplitude that it is unlikely that they result from the action of waves (generated independently somewhere else) on particles. Energetic particles themselves, which are convected from the plasma-sheet towards the dayside outer magnetosphere, must play a fundamental active role in the generation of these waves. Processes involved in such generation mechanisms are briefly reviewed in the next Section.

## 1.5. In situ generation of Pc 4-5 waves

As already noticed, all experimental data do not fit with the theory of Pc 4-5 generation by a Kelvin-Helmotz instability at the magnetopause and subsequent coupling to magnetospheric Alfven waves. The observed periods are not always compatible with the field line resonance theory, the wave polarization is often the result of combined compressional and transverse modes and particle flux modulation is far from being compatible with a simple theory of an adiabatic modification induced by the waves.

Other theories, based upon more or less localized interactions between waves and particles, have been proposed for the generation of the Pc 4-5 waves. In these theories the wave frequency is not imposed by an external source : it does not depend either on the the length of the field line. In some of these theories the wave polarization is imposed, in some others it is a consequence of the interaction*. These theories may be divided into two main categories.

Theories belonging to the first category consist in a sort of macroscopic approach in which the particle distribution functions are characterized by their overall derivatives $\partial F/\partial L$, $\partial F/\partial W$ (where L is the Mc Ilwain parameter and W the particle energy). W varies because of the magnetospheric convection and because of the wave-particle interaction (WPI). The waves are considered to have a pre-established polarization (usually a transverse wave). Following the original ideas of Dungey (1965), this approach has been mainly documented by Southwood (1974, 1976, 1977, 1981).

In the second approach, WPI's are studied by examining the kinetic perturbation of the distribution function in the presence of a wave. The wave characteristics themselves are deduced from the solution of the full dispersion equation. A mixture of cold and hot

* *In all theories $E_{//} = 0$, the cold plasma being sufficiently dense to short-circuit any parallel electric field.*



plasma is introduced, as well as gradients in the hot particle density and in the DC magnetic field. A review of the mathematical techniques and of the physical principles involved in this second approach may be found in Hasegawa's (1975) book.

It is out of the scope of these lectures to go into the details of such theories. However we will illustrate the first approach by discussing the bounce resonance mechanism and the second one by showing the results of some recent theoretical computations (Lin and Parks, 1982).

### Bounce resonance

Let us assume that a standing wave (along the field line) of frequency $\omega$ propagates azimuthally (in the y direction). At any given latitude the phase of the wave field is $\omega t - m\phi$ where $\phi$ is the longitude (measured positively eastward) and m the azimuthal wave number. The longitude of a drifting particle varies like $\omega_d t$ where $\omega_d$ (negative for protons and positive for electrons) is the drift angular frequency. The frequency that the particle sees is Doppler shifted and the apparent frequency of the wave is $\omega - m\omega_d$.

Because of the bounce motion of the particle (with a bounce period $\tau_b = 2\pi/\omega_b$) a cumulative exchange of energy between the particle and the field may occur if the apparent wave frequency is either equal to zero or to an integer multiple of $1/\tau_b$. Resonances occur if

$$\omega - m\omega_d = N\omega_b \qquad (20)$$

where $N = 0, \pm 1, \pm 2, \ldots$

All resonances do not have the same efficiency : as for gyro-resonant interactions (see Chapter 2), the higher the value of N, the lower the efficiency, so that only the lower order resonances are important. Another effect must also be taken into account :

depending on the mode parity, odd or even*, the averaged exchange of energy between the wave and the particle over one bounce period is equal to or different from zero. This is illustrated by Figure 23, the demonstration being given below.

For simplicity reason let us assume that $E_{//} = b_{//} = 0$ and that $\underline{E} = E(z)\,\hat{y}$ where $\hat{y}$ is the unit vector in the azimuthal direction. The instantaneous change of the particle energy

$$\dot{W} = q\,E_{//}\,v_{//} + q\,\underline{E}\cdot\underline{v}_d + \mu\,\partial b_{//}/\partial t \qquad (21)$$

(see for instance Southwood, 1981) is in this case reduced to $Ev_d$ where $v_d$ keeps a constant sign. For an odd mode (left hand part of Figure 23) the sign of E changes when the particle has achieved a quarter of its bounce period. When integrated over one bounce period $\int W\,dt = 0$. For an even mode the situation is different because when the particle crosses the equator the combined effects of the spatial structure of the wave and of its temporal variation are such that the particle sees an electric field which has always the same sign : $\int \dot{W}\,dt \neq 0$. One sees that symmetric modes only resonate with N = 0, $\pm$ 2, ... ; antisymmetric modes resonate with odd orders N = $\pm$ 1, $\pm$ 3, ... (Southwood, 1981).

For the N = 0 order, the field is static (in the reference frame of the particle) and the longitudinal invariant is conserved. The first invariant $\mu$ being always conserved**, there is no first order exchange of energy. Taking all the above arguments into account, one sees that the most important interactions will involve the N = $\pm$ 1 resonances, i.e. antisymmetric modes (second harmonic).

Because $\omega_d$ and $\omega_b$ vary respectively like $v^2$ and v the resonance equation reduces to

$$m\omega_d \approx \omega_b \qquad (22)$$

* *See Figure 3*

** *The wave frequency being much smaller than the gyrofrequency*



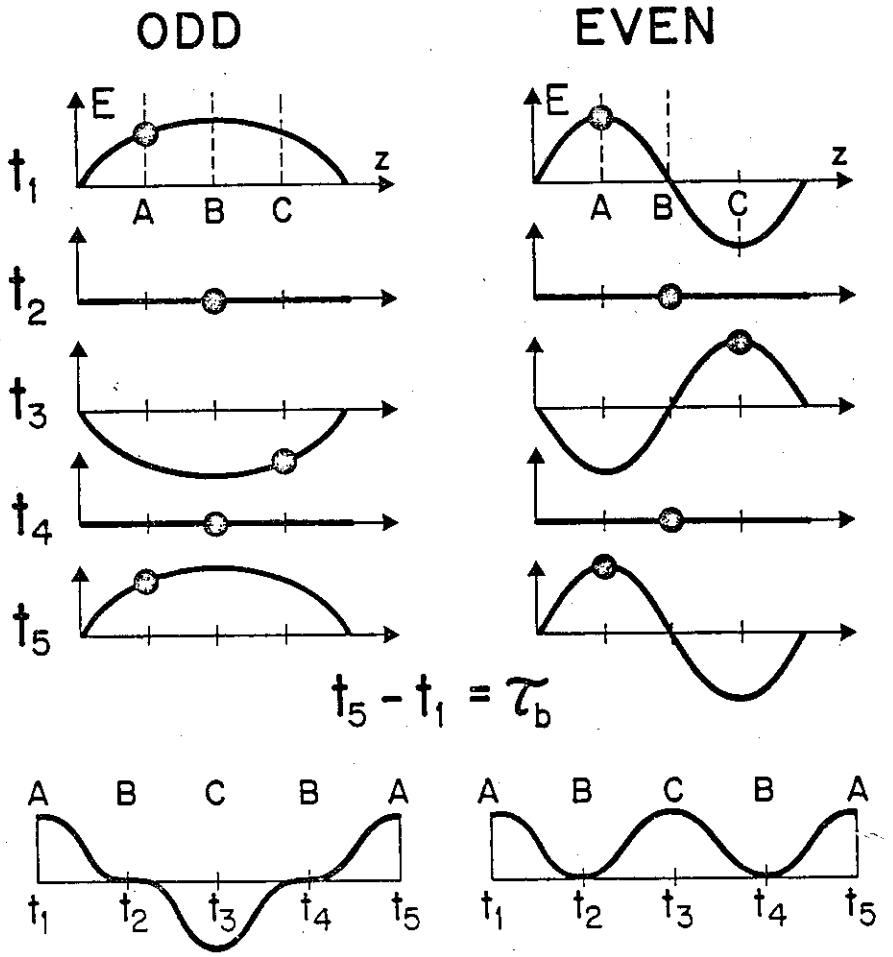


Fig. 23. The bounce resonance phenomenon
The wave frequency (as seen in the frame of the drifting particle) corresponds to the first order resonance N = ± 1. Two wave modes are represented : the fundamental and the second harmonic. In the upper part of the diagram, the field is represented as a function of distance along the field line for different times $t_1$, $t_2$,... The two mirror points of the bouncing particle are A and C. The field seen by the particle in its bouncing motion (heavy dots) is represented on the bottom part of the figure as a function of time.

for particles of high energy (and/or for waves with a high wave number), and to

$$\omega \gtrsim \omega_b \qquad (23)$$

for particles of low energy (and/or for waves with a low wave number). For instance, in order to obtain a wave period of 100 s at L = 6.6, one must consider particles with an energy of 150 keV in the first case (assuming a pich angle $\alpha = 90°$ and $m \sim 40$), and particles of 25 keV (and $\alpha = 0°$) in the second case (i.e. Su et al., 1979). Particles of 25 keV could not satisfy equation (22) except for very high wave numbers ($m \sim 200$).

In a recent paper Southwood and Kivelson (1981) have studied in detail the consequences of such types of interaction on the amplitude and the phase of the particle flux modulation. They showed that these quantities not only depend on the particle energy and pitch angle but also on the value of the density gradient $\partial f/\partial L$ with respect to its adiabatic value $(3W/L)\cdot(\partial f/\partial W)$.

Instability theories

It is out of the scope of this lecture (and out of the competence of its author) to go into the details of such complex plasma theories. It is however important to understand the vocabulary which is used and the physical parameters or mechanisms which are involved.

Usually one considers a hot plasma with a density gradient in the x (radial) direction. The scale length of the density variation is defined by

$$\lambda = \frac{1}{N} \cdot \frac{dN}{dx} \qquad (24)$$

The magnetic field is also assumed to be inhomogeneous :

$$\underline{B} = B_o (1 - \varepsilon x) \hat{z} \qquad (25)$$



From the balance between plasma pressure and magnetic pressure, one easily deduces*

$$\varepsilon = \lambda \beta_{\perp i} / 2 \qquad (26)$$

where $\beta_{\perp i} = \mu_o N m_i U_{\perp i}^2 / B_o^2$ is the ratio of the perpendicular pressure to the magnetic energy density ($m_i U_{\perp i}^2 = 2 \kappa T_{\perp i}$ defines the mean perpendicular temperature of the ion population).** The average velocity of the drift induced by the pressure gradient (see Roederer's lectures) is

$$V_{dP} = \lambda U_{\perp i}^2 / 2 \omega_{ci} \qquad (27)$$

whereas the average magnetic gradient drift velocity (which is in the opposite direction) is

$$V_{dB} = \varepsilon U_{\perp i}^2 / 2\omega_{ci} = V_{dP} \beta_{\perp i} / 2 \qquad (28)$$

In high-β plasmas, the magnetic gradient drift cannot be ignored (Lin and Parks, 1982). The equilibrium distribution function of the hot particles can be expressed as (Hasegawa, 1975) :

$$F = f(v_{//}, v_\perp) \left[ 1 + \lambda \left( x - \frac{v_y}{\omega_{ci}} \right) \right] \qquad (29)$$

where $\omega_{ci} = e B_o / m_i$ is the angular gyrofrequency and where the distribution function f can be assumed to be of the form

$$f(v_{//}, v_\perp) = \frac{N}{(2\pi^3)^{1/2} U_{//i} U_{\perp i}^2} \exp \left[ - \frac{v_{//}^2}{2U_{//}^2} - \frac{v_\perp^2}{U_\perp^2} \right] \qquad (30)$$

The first order perturbation of the distribution function under the influence of a wave can be computed, from which one ceduces the dispersion equation and hence the wave

* *we have neglected here the electron pressure, which is usually smaller than the pressure of ions*

** $m_i$ *is the ion and* $\kappa$ *the Boltzman constant*

polarization characteristics. An example of the results thus obtained for the mirror drift waves is given on Figure 24 (Lin and Parks, 1982). On the left panel the curves have been normalized to

$$\omega^* = - \lambda \, k_\perp U_{\perp i}^2 \, / \, 2\omega_{ci} = - k_\perp V_{dP} \qquad (31)$$

which is the ion drift frequency (due to pressure gradient alone)*. These curves show that the inclusion of the magnetic drift has drastically changed the real part of the dispersion curve and that the growth rate is maximized for waves propagating at large angles to the magnetic field ($k_{//}/k_\perp \sim 0.4$). The right hand part of the figure shows that, for frequencies correponding to the maximum growth rate, the compressional component of the wave is much larger than the transverse one.

The first-order perturbation also gives the average flux variation as a fucntion of the wave field. On Figure 25 the amplitude and the phase of this variation are represented. The amplitude $\psi$ is defined by

$$\psi = (\delta J/J)(B_0/b_z) \qquad (32)$$

The amplitude ratio between the compresional component of the wave and the DC magnetic field has been taken as a normalizing parameter, the amplitude of the modulation being obviously proportional to the amplitude of the wave**. The figure shows that the modulation amplitude is a function of both the particle energy and the particle pitch angle, a result in qualitative agreement with Su et al's (1980) observations. As far as the amplitude is concerned, the agreement is even quantitative : values of $\psi \sim 30$ for $E/T \sim 10$ are to be expected from Su et al's (1980) measurements ($\delta J/J \sim 3$ for $E \sim 150$ keV) assuming that $T \sim 15$ keV and $b_z / B_0 \sim 0.1$ ($b_z \sim 10$nT, $B_0 \sim 100$ nT).

These results show the powerfulness of such theoretical approaches. They also show that more detailed measurements are needed in the field of wave-particle interactions in the long period range.

* *It is easily shown that $\omega^* = - m\omega_{dP}$ since the angular wave number m introduced previously verifies $m = k_\perp \mathcal{R}$ where $\mathcal{R}$ is the equatorial radius of the magnetic shell.*

** *There is obviously a printing error in Lin and Park's (1982) definition of $\psi$ (section 3.b), page 5106).*



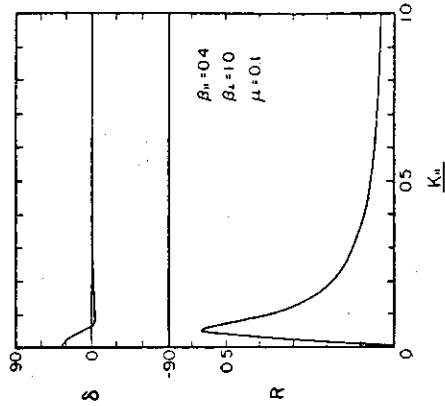


Fig. 24 b. Polarization characteristics of wave shown in Figure 2. $R$ is the ratio of the transverse to the compressional wave amplitude (lower panel); $\delta$ is the relative phase between the transverse and compressional wave component.

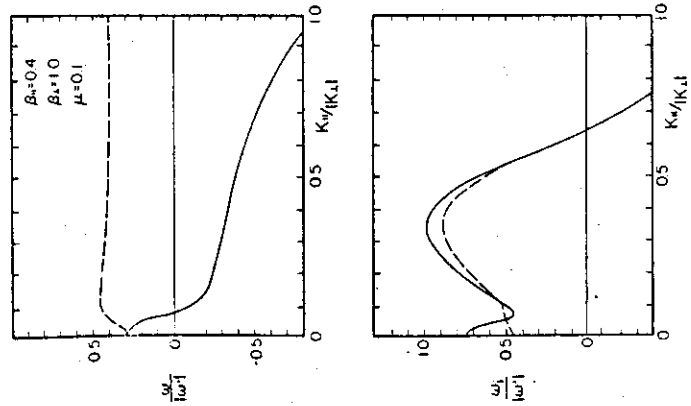


Fig. 24a. Wave frequencies and growth rates normalized by the ion drift frequency as a function of $k_{//}/k_\perp$ for drift mirror Alfvén waves. $N_{//}/N = 0.1$ and $\kappa/k_\perp = 0.1$. The solutions of the dispersion equation with the magnetic gradient effects considered are plotted in solid curves. Dashed curves are solutions without the magnetic gradient effects.

Lin and Parks, J.G.R., 87, 5102, 1982.

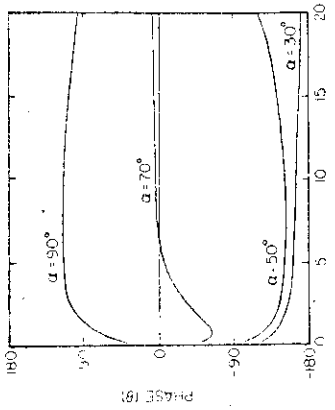


Fig. 25b. Ion flux modulation phase relative to the magnetic field oscillations (compressional component). The abscissa is $E/T_i$. For this figure, the parameters are the same as in Figure 4.

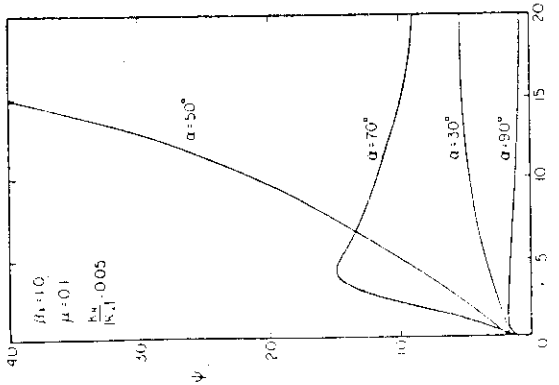


Fig. 25a. Ion flux modulation amplitude $\psi$ as a function of $E/T_i$ at four pitch angles $\alpha$, 30°, 50°, 70°, and 90°. $E$ is the particle total energy and $T_i$ is the particle perpendicular thermal energy. For this figure we use $\omega/|\omega^*| = 0.18$, $\omega/|\omega^*| = 0.49$, $R = 0.57$, $\delta = 8.6°$, and $\beta_i/\beta$ = 2.

Lin and Parks, J.G.R., 87, 5102, 1982.



## 1.6. Conclusion

The huge amount of work devoted to the study of long period pulsations has been paid for. A coherent picture of their propagation characteristics and of their possible excitation mechanisms has emerged. These pulsations are invaluable tools for studying, on a statistical or case by case basis, the generation of waves at the magnetopause boundary or the instabilities in the ring current. These waves also play a fundamental role in the radial diffusion of energetic particles (i.e. Schulz and Lanzerotti, 1974 ; Lanzerotti et al., 1978) and they contribute by a non negligible amount to the energy budget of magnetospheric processes (Greenwald and Walker, 1980)*. On the contrary the use of the long period pulsations for the quantitative diagnosis of the magnetopsheric or solar wind plasma, which has been advocated by many people, is - to the author's opinion - based on grounds which are not solid enough to be worth the effort, taking into account all the unknown intervening parameters.

* *The Joule heating due to pulsations in $\sim 5 \times 10^{16}$ erg. $s^{-1}$, to be compared with the energy deposited by particle precipitation ($2 \times 10^{17} - 10^{18}$), ionospheric currents ($2 \times 10^{17} - 10^{18}$), auroral luminosity ($10^{16} - 10^{17}$) or kilometric radiation ($10^{14} - 10^{16}$).*

# REFERENCES TO CHAPTER 1


## BOOKS

GUL'ELMI, A.V., 'MHD Waves in the Near Earth Magnetosphere', Nauka, Moscow, 1979 (in Russian).

GUL'ELMI, A.V., and V.A. TROITSKAYA, 'Geomagnetic Pulsations and Diagnostics of the Magnetosphere', Nauka, Moscow, 1973 (in Russian).

JACOBS, J.A., 'Geomagnetic Pulsations', Springer-Verlag, Berlin, 1970.

HASEGAWA, A., 'Plasma Instabilities and Non linear Effects', Springer-Verlag, New-York, 1975.

NISHIDA, A., 'Geomagnetic Diagnosis of the Magnetosphere', Springer-Verlag, New-York, 1978.

SCHULZ, M., and L.J. LANZEROTTI, 'Particle Diffusion in the Radiation Belts', Springer-Verlag, Berlin, 1974.

SOUTHWOOD, D.J. (Editor), 'ULF Pulsations in the Magnetosphere', Proceedings of the Special Sessions on Geomagnetic Pulsations at XVII General Assembly of the International Union for Geodesy and Geophysics, Canberra, 1979, December, D. Reidel Pub., Dordrecht, 1981. Hereafter referenced as "ULF Pulsations ..."

## REVIEWS

DUNGEY, J.W., The structure of the exosphere or adventures in velocity space, in 'Geophysics, the Earth's Environment', C. De Witt, J. Hiéblot, A. Lebeau eds., Gordon and Breach, New-York, 1963, pp. 401-550.





DUNGEY, J.W., Effects of electromagnetic perturbations on particles trapped in the radiation belts. Space Sci. Rev., 4, 199-222, 1965.

DUNGEY, J.W., Hydromagnetic waves, in 'Physics of Magnetospheric Phenomena', Vol. 11, S. Matsushita and W. Campbell eds., Academic Press, New-York, 1967, pp. 913-934.

GENDRIN, R., Waves and wave-particle interactions in the magnetosphere, Space Sci. Rev., 18, 145-200, 1975.

GREENSTADT, E.W., R.L. Mc PHERRON and K. TAKAHASHI, Solar wind control of daytime, midperiod geomagnetic pulsations, in 'ULF Pulsations ...', 1981, pp. 89-110.

GUL'ELMI, A.V., Diagnostics of the magnetosphere and interplanetary medium by means of pulsations, Space Sci. Rev., 16, 331-344, 1974.

HASEGAWA, A., and L. CHEN, Theory of magnetic pulsations, Space Sci. Rev., 16, 347-359, 1974.

HUGHES, W.J., Multisatellite observations of geomagnetic pulsations, in 'ULF Pulsations ...', 1981, pp. 41-55.

KNOX, F.B., and W. ALLAN, Damping and coupling of long-period hydromagnetic waves by the ionosphere, in 'ULF Pulsations...', 1981, pp. 129-139.

KOKUBUN, S., Observations of Pc pulsations in the magnetosphere : Satellite-ground correlation, in 'ULF Pulsations ...', 1981, pp. 17-39.

LANZEROTTI, L.J., and D.J. SOUTHWOOD, Hydromagnetic waves, in 'Solar System Plasma Physics', Vol. 3, L.J. Lanzerotti, C.F. Kennel and E.N. Parker eds., North-Holland, Netherlands, 1979, pp. 110-135.

ORR, D., Magnetic pulsations within the magnetosphere : a review, J. Atmos. Terrest. Phys., 35, 1-50, 1973.

SOUTHWOOD, D.J., Recent studies in micropulsation theories, Space Sci. Rev., 16, 413-425, 1974.

SOUTHWOOD, D.J., Low frequency pulsation generation by energetic particles, in 'ULF Pulsations ...,' 1981, pp. 75-88.

WALKER, A.D.M., and R.A. GREENWALD, Pulsation structure in the ionosphere derived from auroral radar data, in 'ULF Pulsations...', 1981, pp. 111-127.

OTHER REFERENCES CITED IN THE TEXT

ANDREWS, M.K., L.J. LANZEROTTI and C.G. MACLENNAN, The rotation of hydromagnetic waves by the ionosphere, in 'ULF Pulsations...', 1981, pp. 141-145.

ARTHUR, C.W., R.L. Mc PHERRON, L.J. LANZEROTTI and D.C. WEBB, Geomagnetic field fluctuations at synchronous orbit, 1. Power spectra, J. Geophys. Res., 83, 3859-3865, 1978.

BAXTER, D. and R.E. LAQUEY, Plasma oscillations at 2-3 millihertz at 6.6 Earth Radii, J. Geophys. Res., 78, 6798-6801, 1973.

CAVACIUTI, N., F. GLANGEAUD et J.L. LACOUME, Détermination de la densité de protons de la magnétosphère à partir d'observations des pulsations géomagnétiques de type Pc3, C.R. Acad. Sci., 276 B, 631-634, 1973.

CHEN, L., and A. HASEGAWA, A theory of long period magnetic pulsations,
1. Steady state excitation of field line resonance, J. Geophys. Res., 79, 1024-1032, 1974.
2. Impulse excitation of surface eigenmode, J. Geophys. Res., 79, 1033-1037, 1974.



ENGEBRETSON, M.J., and L.J. CAHILL, Jr., Pc5 pulsations observed during the June 1972 geomagnetic storm, J. Geophys. Res., 86, 5619-5631, 1981.

GREENSTADT, E.W., H.J. SINGER, C.T. RUSSEL and J.V. OLSON, IMF orientation, solar wind velocity and Pc 3-4 signals : A joint distribution, J. Geophys. Res., 84, 527-532, 1979.

GREENWALDT, R.A., and A.D.M. WALKER, Energetics of long period resonant hydromagnetic waves, Geophys. Res. Lett., 7, 745-748, 1980.

GUL'ELMI, A.V., T.A. PLYASOVA-BAKUNINA and R.V. SHCHEPETNOV, Relation between the period of geomagnetic pulsations Pc 3-4 and the parameters of the interplanetary medium at the Earth's orbit, Geomagn. Aeron., 13, 331-333, 1973.

HASEGAWA, A., and L.J. LANZEROTTI, On the orientation of hydromagnetic waves in the magnetosphere, Rev. Geophys. Space Phys., 16, 263-266, 1978.

HIGEL, B., and W. LEI, Electron density and plasmapause characteristics at 6.6 Re : a statistical study of the GEOS-2 relaxation sounder data, J. Geophys. Res., to be published, 1982.

HUGHES, W.J., and D.J. SOUTHWOOD, The screening of micropulsation signals by the atmosphere and ionosphere, J. Geophys. Res., 81, 3234-3240, 1976 a.

HUGHES, W.J., and D.J. SOUTHWOOD, An illustration of modification of geomagnetic pulsation structure by the ionosphere, J. Geophys. Res., 81, 3241-3247, 1976 b.

HUGHES, W.J., R.L. Mc PHERRON and J.N. BARFIELD, Geomagnetic pulsations observed simultaneoustly on three geostationnary satellites, J. Geophys. Res., 83, 1109-1116, 1978.

HUGHES, W.J., R.L. Mc PHERRON, J.N. BARFIELD and B.H. MAUK, A compressional Pc 4 pulsation observed by three satellites in geostationary orbit near local midnight, Planet. Space Sci., 27, 821-840, 1979.

KOKUBUN, S., M.G. KIVELSON, R.L. Mc PHERRON, C.T. RUSSEL and H.I. WEST, Jr., OGO 5 observations of Pc 5 waves : particle flux modulations, J. Geophys. Res., 82, 2774-2786, 1977.

KREMSER, G., A. KORTH, J.A. FEJER, B. WILKEN, A.V. GUREVITCH and E. AMATA, Observations of quasi-periodic flux variations of energetic ions and electrons associated with Pc 5 geomagnetic pulsations, J. Geophys. Res., 86, 3345-3356, 1981.

LANZEROTTI, L.J., D.C. WEBB and C.W. ARTHUR, Geomagnetic field fluctuations at synchronous orbit, 2. Radial diffusion, J. Geophys. Res., 83, 3866-3870, 1978.

LAQUEY, R.E., Observation of collisionless driftwaves, Phys. Fluids, 16, 550-558, 1973.

LATHUILLIERE, C., F. GLANGEAUD, J.L. LACOUME and G. LEJEUNE, Relationship between ionospheric electric field and ground magnetic pulsation in the Pc 3 domain at midlatitude, J. Geophys. Res., 86, 7669-7678, 1981.

LIN, C.L., and G.K. PARKS, The coupling of Alfven and compressional waves, J. Geophys. Res., 83, 2628-2636, 1978.

LIN, C.S., and G.K. PARKS, Modulation of energetic particle fluxes by a mixed mode of transverse and compressional waves, J. Geophys. Res., 87, 5102-5108, 1982.

NAGATA, T., S. KOKUBUN and T. IIJIMA, Geomagnetically conjugate relationships of giant pulsations at Syowa Base, Antarctica and Rejkjavik, Iceland, J. Geophys. Res., 68, 4621-4625, 1963.



OLSON, J.V., and G. ROSTOKER, Longitudinal phase variations of Pc 4-5 micropulsations, J. Geophys. Res., 83, 2481-2488, 1978.

SAITO, T., T. SAKURAI and T. TAMURA, Study of magnetospheric disturbances based on a high-speed analysis of ULF waves, Proc. IMS Symp. held at ISAS, Tokyo Univ., July 1976, pp. 6-17.

SAMSON, J.C., J.A. JACOBS and G. ROSTOKER, Latitude-dependent characteristics of long period geomagnetic micropulsations, J. Geophys. Res., 76, 3675-3683, 1971.

SAMSON, J.C. and G. ROSTOKER, Latitude-dependent characteristics of high-latitude Pc 4 and Pc 5 micropulsations, J. Geophys. Res., 77, 6133-6144, 1972.

SINGER, H.J., D.J. SOUTHWOOD, R.J. WALKER and M.G. KIVELSON, Alfven wave resonances in a realistic magnetospheric magnetic field geometry, J. Geophys. Res., 86, 4589-4596, 1981.

SINGER, H.J., W.J. HUGHES and C.T. RUSSEL, Standing hydromagnetic waves observed by ISEE 1 and 2 : radial extent and harmonic, J. Geophys. Res., 87, 3519-3529, 1982.

SOUTHWOOD, D.J., Some features of field line resonances in the magnetosphere, Planet. Space Sci., 22, 483-491, 1974.

SOUTHWOOD, D.J., A general approach to low frequency instability in the ring current plasma, J. Geophys. Res., 81, 3340-3348, 1976.

SOUTHWOOD, D.J., Localised compressional hydromagnetic waves in the magnetospheric ring current, Planet. Space Sci., 25, 549-554, 1977.

SOUTHWOOD, D.J., and M.G. KIVELSON, Charged particle behaviour in low frequency geomagnetic pulsations, 1. Transverse waves, J. Geophys. Res., 86, 5643-5655, 1981.

STUART, W.F., and L.J. LANZEROTTI, Long period hydromagnetic waves inside the plasmasphere, J. Geophys. Res., 87, 1703-1706, 1982.

SU, S.-Y., A. KONRADI and T.A. FRITZ, On propagation direction of ring current proton ULF waves observed by ATS 6 at 6.6 Re, J. Geophys. Res., 82, 1859-1868, 1977.

SU, S.-Y, A. KONRADI and T.A. FRITZ, On energy dependent modulation of the ULF ion flux oscillations observed at small pitch angles, J. Geophys. Res., 84, 6510-6516, 1979.

SU, S.-Y, R.L. Mc PHERRON, A. KONRADI and T.A. FRITZ, Observations of ULF oscillations in the ion fluxes at small pitch angle with ATS, J. Geophys. Res., 85, 515-522, 1980.

TAKAHASHI, K., and R.L. Mc PHERRON, Harmonic structure of Pc 3-4 pulsations, J. Geophys. Res., 87, 1504-1516, 1982.

VERÖ,J., and L. HOLLÖ, Connections between interplanetary magnetic field and geomagnetic pulsations, J. Atmos. Terres. Phys., 40, 857-865, 1978.

VILLAIN, J.P., Characteristics of Pc-5 micropulsations as determined with the STARE experiment, J. Geophys. Res., 87, 129-137, 1982.

WALKER, A.D.M., R.A. GREENWALD, W.F. STUART and C.A. GREEN, STARE auroral radar observations of Pc 5 geomagnetic pulsations, J. Geophys. Res., 84, 3373-3388, 1979.



# APPENDIX A

## WAVE PROPAGATION IN A COLD MAGNETOPLASMA AT ULF AND VLF FREQUENCIES

### A.1 General formulae

The dispersion equation for waves propagating in magnetoplasmas can be found in every textbook on Plasma Physics (i.e. Ratcliffe, 1959 ; Budden, 1961 ; Stix, 1962 ; Quémada, 1968)*. We recall it here in order to ensure the homogeneity of the notations and to introduce simplified expressions for waves propagating in the 'whistler mode' ($f < f_{ce}$) or in the 'hydromagnetic regime' ($f < f_{ci}$). Let us introduce :

$$X_h = \frac{q_h^2 N_h}{\varepsilon_o m_h} \frac{1}{\omega^2} \qquad Y_h = \frac{q_h B}{m_h} \frac{1}{\omega} \tag{A.1}$$

where $N_h$ is the number of particles of species h per unit volume, $m_h$ and $q_h$ their mass and charge (positive for positive ions and negative for electrons). Let us introduce also the relative masses of the ions with respect to the electrons, $m_i^*$ and the concentration ratio $A_i$ of each ions species (one assumes that there is no negative ions) :

$$N_i = N_e A_i \qquad \text{with} \qquad \sum_i A_i = 1 \tag{A.2}$$

so that

$$\left.\begin{aligned} X_i &= \frac{A_i X_e}{m_i^*} & Y_i &= -\frac{Y_e}{m_i^*} \\ X_e &= \left(\frac{\omega_{pe}}{\omega}\right)^2 & Y_e &= -\frac{\omega_{ce}}{\omega} \end{aligned}\right| \tag{A.3}$$

where $\omega_{pe}$ and $\omega_{ce}$ are the electron plasma frequency and gyrofrequency.

* *One may find in a simple and elegant demonstration of the wave properties in a paper by Smith and Brice (1964), whose formalism is used here.*

There exist three principal limiting modes for which there is no fluctuation in the electron density, i.e. for which :

$$\underline{\nabla} \cdot \underline{E} = 0 \quad \text{or} \quad \underline{k} \cdot \underline{E} = 0 \tag{A.4}$$

Two of them are circularly polarized, their electric and magnetic vectors are perpendicular to $\underline{k}$, the other being linearly polarized, also in the wave front. These three modes are defined by the suffix $s(=+1,-1,0)$, their phase indices are defined by :

$$\mu_s^2 = 1 - \sum_h \frac{X_h}{sY_h + 1} \tag{A.5}$$

and their phase velocities by :

$$W_s = c/\mu_s \tag{A.6}$$

If condition (A.4) is released, one finds the general dispersion equation, or the 'tangent equation' :

$$(W^2 - W_e^2)(W^2 - W_o^2)\sin^2\theta + (W^2 - W_{+1}^2)(W^2 - W_{-1}^2)\cos^2\theta = 0 \tag{A.7}$$

where $\theta$ is the wave normal angle, $(\underline{k}, \underline{B})$ and where a new velocity has been introduced.

$$W_e^2 = \frac{1}{2}(W_{+1}^2 + W_{-1}^2) \tag{A.8}$$

Equation (A.7) can be transformed in the usual biquadratic form :

$$W^4 - W^2\left[(W_o^2 - W_e^2)\sin^2\theta + 2W_e^2\right] + W_e^2 W_o^2 \sin^2\theta + W_{+1}^2 W_{-1}^2 \cos^2\theta = 0 \tag{A.9}$$

from which one deduces

$$W_{\pm}^2 = W_e^2 + \frac{1}{2}(W_o^2 - W_e^2)\sin^2\theta \pm \frac{1}{2}\sqrt{(W_o^2 - W_e^2)^2 \sin^4\theta + (W_{+1}^2 - W_{-1}^2)^2 \cos^2\theta} \tag{A.10}$$

For each wave normal direction, two waves can propagate, one of them being possibly evanescent ($W^2 < 0$). For $\theta = 0$, one finds the two principal circularly polarized modes

$$W_+^2 = W_{+1}^2 \qquad W_-^2 = W_{-1}^2 \tag{A.11}$$



For $\theta = \pi/2$, one finds the ordinary mode (also circularly polarized) : $W_+^2 = W_o^2$ (but this mode is evanescent for frequencies below the plasma frequency) and the extraordinary mode :

$$W_-^2 = W_e^2 \tag{A.12}$$

An example of the frequency dependence of the phase velocity for the three principal modes in the VLF and ULF ranges is given on Figure A.1 which is drawn for a plasma containing two ion species (66% of $H^+$ and 33% of $He^+$). Resonance frequencies ($W = 0$) and cut-off frequencies ($W \to \infty$) are clearly evidenced on this figure.

Depending on the relative importance of the two terms under the square-root sign, expression (A.10) can be simplified, leading to the quasi-longitudinal (QL) and to the quasi-transverse (QT) approximations. The first one is valid when :

$$(W_o^2 - W_e^2)^2 \sin^4\theta \ll (W_{+1}^2 - W_{-1}^2)^2 \cos^2\theta \tag{A.13}$$

the second one when

$$(W_o^2 - W_e^2)^2 \sin^4\theta \gg (W_{+1}^2 - W_{-1}^2)^2 \cos^2\theta \tag{A.14}$$

The domains of validity of the QL and QT approximations depend on the frequency range and of the ratio $X_e / Y_e^2 = \left(f_{pe} / f_{ce}\right)^2$ (see section A.3). When collisions are introduced they are also determined by the ratio $\nu/\omega_c$ where $\nu$ is the collision frequency (section A.5). The QL approximation may be valid up to large wave normal angles ; conversely, it may occur that the QT approximation can be used even for small values of $\theta$ (Section A.3 and 2.2).

## A.2 Correspondence with other notations

Instead of using phase velocities, other notations make use of the indices. For instance, Stix's (1962) notations, which are often used are :

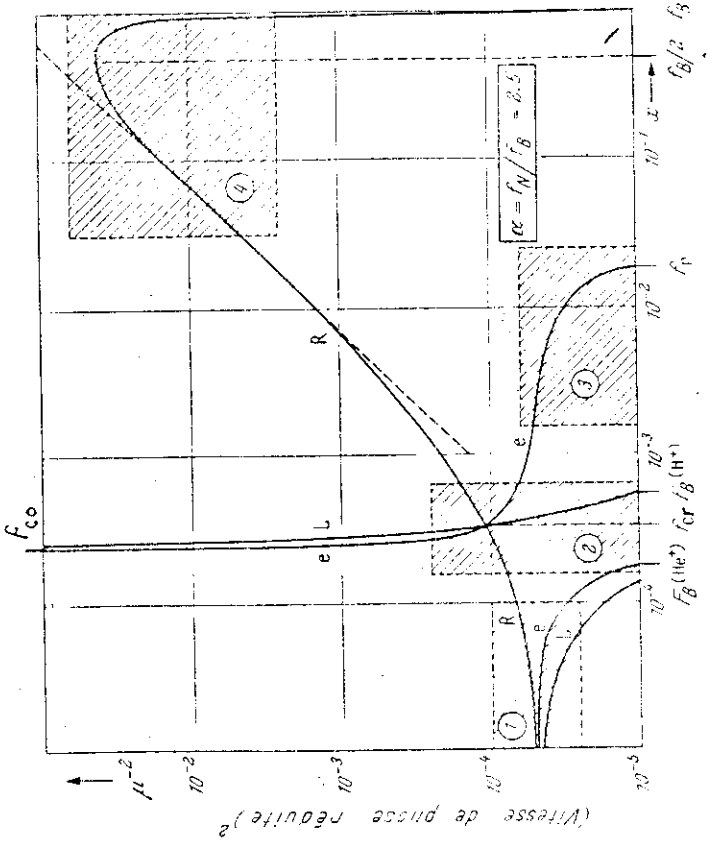


Fig. A.1 Variation de la vitesse de phase réduite ($1/\mu^2$) en fonction de la fréquence réduite ($x = f/|Y_e| = f/f_B$) pour un plasma à deux constituants ioniques, à savoir $H^+$ (66%) et $He^+$ (33%); $\alpha = X^{\frac{1}{2}}/|Y_e| = f_{pi}/f_B$ précise la densité électronique réduite. On a représenté les deux modes qui se propagent parallèlement au champ magnétique, de polarisation circulaire droite (R) et gauche (L) et le mode extraordinaire (e) qui se propage transversalement. En pointillé, l'approximation d'Appleton-Storey pour le mode droit. Les zônes hachurées représentent les quatre régions du plan bien séparées par quatre types de phénomènes exosphériques particuliers. (Adapté de Smith et Brice [61])

Gendrin, in "Handbuch der Physik", vol. 49, p. 1, Springer Verlag, 1972, pp. 401-525.



$$
\begin{aligned}
R &= \mu_{+1}^2 \\
L &= \mu_{-1}^2 \\
P &= \mu_0^2 \\
S &= \frac{1}{2}(R+L)
\end{aligned}
\qquad \text{(A.15)}
$$

The use of these parameters is not so practical because resonances ($W \to 0$) and cut-offs ($W \to \infty$) are not obtained for the same limiting values. For instance cut-offs are obtained for $R = 0$, $L = 0$, $P = 0$, but the cut-offs for the transverse mode are not defined by $S = 0$ but by $S = R/2$ or $S = L/2$. On the contrary $S = 0$ defines the resonance of the transverse mode (the hybrid resonance) whereas the two other resonances (the gyroresonances) are obtained for $R \to \infty$ or $L \to \infty$.

One also finds in the literature the biquadratic equation for the index of refraction*

$$AN^4 - BN^2 + C = 0 \qquad \text{(A.16)}$$

with

$$
\begin{aligned}
A &= S\sin^2\theta + P\cos^2\theta \\
B &= RL\sin^2\theta + PS(1+\cos^2\theta) \\
C &= PRL
\end{aligned}
\qquad \text{(A.17)}
$$

The shape of the velocity surfaces is different in each region of the Clemmow-Mullaly-Allis (CMA) diagram which is represented on Figure A.2 (Note that the y coordinate is equal to $Y_e^2$).

Instead of using the parameters $X_h$ and $Y_h$ defined by (A.3) it is often more advantageous to introduce other dimensionless parameters such as

$$\alpha = f_{pe} / f_{ce} \qquad \text{(A.18)}$$

which defines the medium and

$$x = f/f_{ce} \quad \text{or} \quad X = f/f_{ci} \qquad \text{(A.19)}$$

* *Obviously its solution has a less simple form than (A.10).*

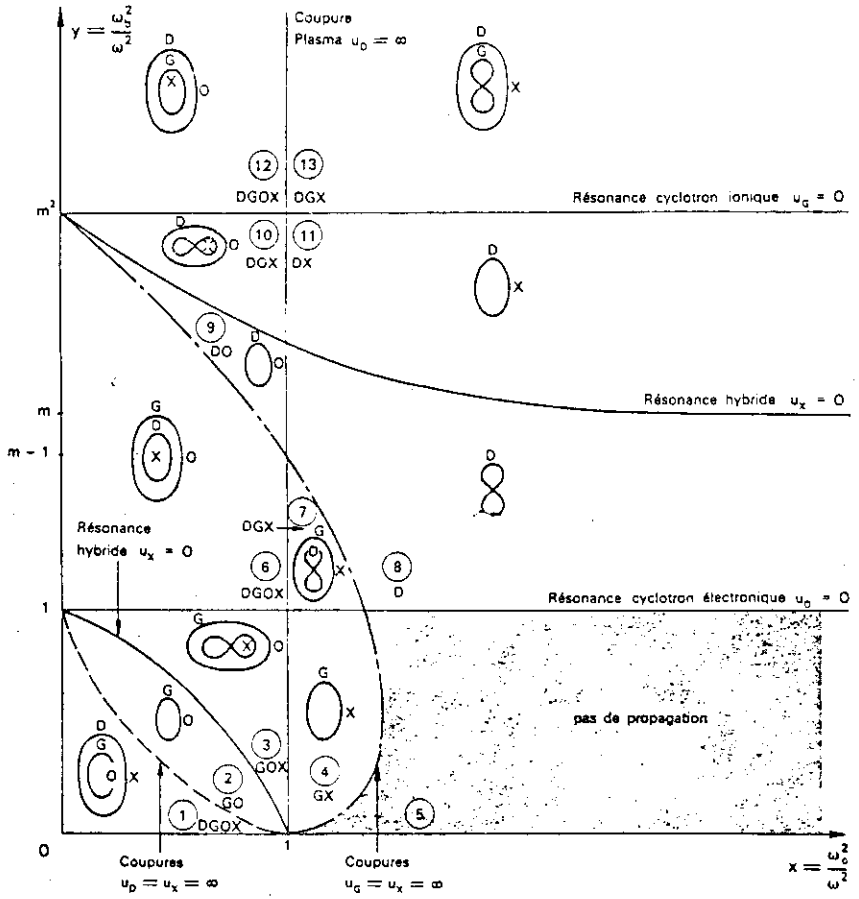


Fig. A.2. C.M.A. diagram. The phase velocities are represented by the symbol u, with the following correspondence with the text notation : $u_D \equiv W_{+1}$, $u_G \equiv W_{-1}$, $u_O \equiv W_O$, $u_X \equiv W_e$. Cut-offs ('coupures' in French) obtained for R = 0 (or L = 0) in Stix's notation correspond to $u_D = \infty$ (or $u_G = \infty$) and $u_x = \infty$. The cut-off at the plasma frequency ($u_O = \infty$) corresponds to P = 0. Gyroresonances are obtained for $u_D$ or $u_G = 0$ (R or L = $\infty$)and hybrid resonance for $u_x = 0$ (S = 0). The diagrams which are drawn into each CMA region give the shapes of the phase velocity curves as a function of wave normal angle (the DC magnetic field is in the direction of the y axis). m is the mass ratio between ions and electrons (one component plasma). After Quémada, 1968.



which characterize the frequency. The parameter x will be used in the study of VLF waves (x < 1) and X in the study of ULF waves (X < 1). In the magnetosphere, $\alpha$ is usually larger than 1, except in the hight altitude ($\sim 1\ R_e$) auroral regions ($\Lambda \sim 65°$). Approximation which can be obtained in these conditions are discussed in the next section.

## A.3. Approximations valid in the ULF and VLF ranges

We restrict ourselves to the case $\alpha^2 \gg 1$, although some formulae are also valid when this condition is not satisfied. In the VLF range, for x < 1, one obtains :

$$\left.\begin{aligned} W_{+1}^2 &= \frac{c^2}{\alpha^2}\ (1 - x)\ (\frac{1}{m^*} + x) \\ W_{-1}^2 &= \frac{c^2}{\alpha^2}\ (1 + x)\ (\frac{1}{m^*} - x) \\ W_O^2 &= -\frac{c^2}{\alpha^2}\ x^2 \\ W_e^2 &= \frac{c^2}{\alpha^2}\ (\frac{1}{m^*} - x^2) \end{aligned}\right| \qquad (A.20)$$

which lead to the following dispersion relation

$$\frac{W_\pm\ \alpha^2}{c^2} = \frac{1}{m^*}\ (1 - \frac{1}{2}\sin^2\theta) - x^2 \pm \sqrt{\frac{\sin^4\theta}{4m^{*2}} + x^2\cos^2\theta} \qquad (A.21)$$

In these expressions, which are valid for a plasma containing only one ion species, $m^* = m_i/m_e$ (= 1840 for a proton plasma) has been neglected when compared to 1.

The lower hybrid frequency $f_{\ell hr}$ is defined by $W_e = 0$, i.e.

$$x_{\ell hr}^2 = \frac{1}{m^*} \quad \text{or} \quad f_{\ell hr}^2 = f_{ce} \cdot f_{ci} \qquad (A.22)$$

It defines two frequency ranges : the VLF range ($x^2 \gg 1/m^*$) and the ULF range ($x^2 \ll 1/m^*$ or $X^2 \ll m^*$). In the VLF range (so defined), the dispersion equation becomes even more simplified, leading to only one mode, the whistler mode :

$$W_+ = \frac{c}{\alpha} x^{1/2} (\cos\theta - x)^{1/2} \qquad (A.23)$$

the mode $W_-$ being evanescent ($W^2_- < 0$).

In the ULF range ($X^2 << m^*$), one has :

$$\left.\begin{aligned} W_{+1}^2 &= V_A^2 (1+X) \\ W_{-1}^2 &= V_A^2 (1-X) \\ W_o^2 &= 0 \\ W_e^2 &= V_A^2 \end{aligned}\right| \qquad (A.24)$$

where

$$V_A^2 = c^2/(\alpha^2 m^*) \qquad (A.25)$$

is the Alven velocity, as can be seen from the definitions of $\alpha$ and $m^*$. Equations (A.10) and (A.24) give*

$$W_\pm^2 = V_A^2 \left\{ 1 - \frac{1}{2}\sin^2\theta \pm \frac{1}{2}\sqrt{\sin^4\theta + 4X^2\cos^2\theta} \right\} \qquad (A.26)$$

This expression can still be simplified but one must be careful. The QT approximation, which is valid for very low frequencies over a wide range of angular directions** easily gives

$$W_+ = V_A \qquad (A.27)$$

$$W_- = V_A \cos\theta \qquad (A.28)$$

The first mode is the isotropic Alfven mode ; the second one, which is very anisotropic, is the modified Alfven mode. The QL approximation

$$W_\pm^2 = V_A^2 \left[ 1 - \frac{1}{2}\sin^2\theta \pm X\cos\theta \right] \qquad (A.29)$$

* *One could also use directly (A.21.)*

** *When X = 0.1 for instance, condition (A.4) is satisfied for 30°<θ<90°. When X = 0.3, condition (A.12) is satisfied for 0<θ<30°*



should be in principle also valid over a wide range of angles at higher frequencies*. However, it is dangerous to use it : it is valid for $W_+$ but not for $W_-$ when the frequency approaches the resonance frequency. For instance, by using the complete expression (A.26), one easily finds that the resonance ($W_- = 0$) occurs at $X = 1$ whatever $\theta$, whereas (A.29) does give resonances for $\cos\theta = X - \sqrt{X^2 - 1}$ which would mean that X should be larger than 1. This is because terms of second order in $\theta$, which are necessary to include near the resonance, have been omitted in (A.29).

In the range of small $\theta$ values there is only one approximation which is useful. It is the one which corresponds to strictly longitudinal propagation :

$$W_\pm^2 = V_A^2 (1 \pm X) \qquad (A.30)$$

When $\theta$ is not strictly equal to zero, one must use the complete expression (A.26), at least for the anisotropic mode.

## A.4. Polarization

The polarization is characterized by quantities proportionnal to $E_x$, $E_y$, $E_z$ where the axes are defined on Figure A.3, $\hat{k}$, $\hat{x}$ and $\hat{z}$ being coplanar and $\hat{z}$ being parallel to the static magnetic field $\underline{B}$. One has (see f.i. Smith and Brice, 1964) :

$$\left.\begin{aligned} E_x &\propto \frac{\sin\theta}{2}\left[\frac{W_{+1}^2}{W_{+1}^2 - W^2} + \frac{W_{-1}^2}{W_{-1}^2 - W^2}\right] \\ iE_y &\propto \frac{\sin\theta}{2}\left[\frac{W_{+1}^2}{W_{+1}^2 - W_{-1}^2} - \frac{W_{-1}^2}{W_{-1}^2 - W^2}\right] \\ E_z &\propto \cos\theta \left[\frac{W_o^2}{W_o^2 - W^2}\right] \end{aligned}\right| \qquad (A.31)$$

* *When X = 0.1 for instance, condition (A.4) is satisfied for 30°<θ<90°. When X = 0.5, condition (A.13) is satisfied for 0<θ<30°.*

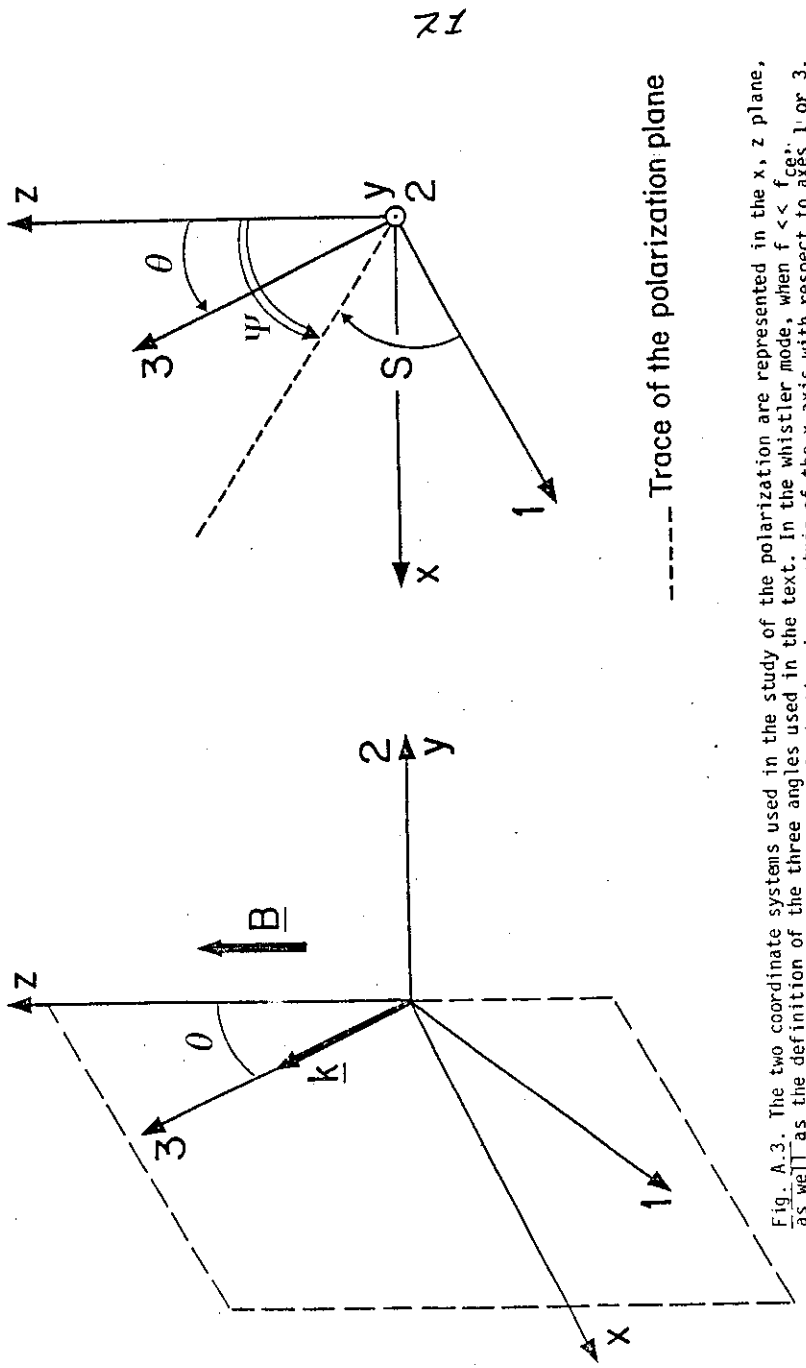


----- Trace of the polarization plane

Fig. A.3. The two coordinate systems used in the study of the polarization are represented in the x, z plane, as well as the definition of the three angles used in the text. In the whistler mode, when $f << f_{ce}$, $S = -\theta$ so that the trace of the plane of polarization is symmetric of the x axis with respect to axes 1 or 3.



The two first expressions can be transformed into a less symmetric but more useful form

$$\left.\begin{aligned} E_x &\propto \sin\theta \; \frac{(W_{+1}^2 W_{-1}^2 - W^2 W_e^2)}{(W_{+1}^2 - W^2)(W_{-1}^2 - W^2)} \\ iEy &\propto \cdot \frac{\sin\theta}{2} \; \frac{W^2(W_{-1}^2 - W_{+1}^2)}{(W_{+1}^2 - W^2)(W_{-1}^2 - W^2)} \end{aligned}\right| \qquad (A.32)$$

Because $E_x/E_z$ is real, the electric field vector lies in a phase normal to the xz plane, which is the plane of polarization. Its orientation is defined by

$$\tan\psi = E_x/E_z \qquad (A.33)$$

The polarization ellipse is then completely defined by the ratio $E_y/E_x$. However it is better to use another coordinate system where axis 3 is along $\underline{k}$, axis 2 is identical to $\hat{y}$ and axis 1 is in the x, z plane. Such a choice is interesting because the magnetic field of the wave $\underline{b}$, which lies in the 1, 2 plane because $\underline{k} \cdot \underline{b} = 0$, is simply obtained by a rotation of $\underline{E}_\perp$, $\underline{E}_\perp$ being the component of $\underline{E}$ in the wavefront (the 1, 2 plane) :

$$\underline{b} = \frac{1}{\omega} \; \underline{k} \times \underline{E}_\perp \qquad (A.34)$$

The polarization is defined by the ratio

$$\rho = E_2/E_1 \qquad (A.35)$$

The transformation formulae between the two coordinate systems are :

$$\left.\begin{aligned} E_1 &= E_x \cos\theta - E_z \sin\theta \\ E_2 &= E_y \\ E_3 &= E_x \sin\theta + E_z \cos\theta \end{aligned}\right| \qquad (A.36)$$

from which one deduces, with the help of (A.31) for Ez and (A.32) for $E_x$ :

$$E_1 \propto \frac{\sin\theta \cos\theta\, W^4 \left[ W^2(W_e^2 - W_o^2) + W_o^2 W_e^2 - W_{+1}^2 W_{-1}^2 \right]}{(W_o^2 - W^2)(W_{+1}^2 - W^2)(W_{-1}^2 - W^2)} \qquad (A.37)$$

The similar expression for $E_3$ is of no use, the plane of polarization being defined by (A.33) as well as by the ratio $E_1/E_3$.

A much more simple expression for $E_1$ is obtained by replacing the product $W_{+1}^2 W_{-1}^2$ by its value as deduced from (A.9). One obtains

$$E_1 \propto \frac{\sin\theta}{\cos\theta} \frac{W^2(W_e^2 - W^2)}{(W_{+1}^2 - W^2)(W_{-1}^2 - W^2)} \qquad (A.38)$$

from which one deduces

$$\rho_{\pm} = \frac{\cos\theta}{2i} \frac{W_{+1}^2 - W_{-1}^2}{W_{\pm}^2 - W_e^2} \qquad (A.39)$$

where $W_{\pm}$ is given by (A.10). By using this same equation one easily demonstrates that

$$\rho_+ \cdot \rho_- = 1 \qquad (A.40)$$

The polarizations of the two waves which can propagate in a given direction $\rho$ with the same frequency f are inverse.

These results can be used for studying the polarization of VLF and ULF waves by making some approximations. In the limit $\alpha^2 \gg 1$ and $x^2 \gg 1/m^*$ the use of equations (A.20) (A.32) (A.33) and (A.33) leads to

$$\rho_+ = -i \qquad (A.41)$$

and

$$\tan\psi = \frac{1 - x\cos\theta}{x\sin\theta} \qquad (A.42)$$



Equation (A.41) shows that the whistler mode (the only one which can propagate for $m^{*-1/2} < x < 1$) is right hand polarized. Equation (A.42) is different from the equation given by Storey (1959), which is valid only for $x \ll 1$.* It shows that, for small $\theta$, the plane of polarization is almost perpendicular to B. When the wave normal approaches the resonance cone ($\theta \to \cos^{-1}x$) the polarization plane almost contains the wave normal direction. Because the polarization in the plane perpendicular to k is still circular, the components $E_2$ and $E_1 \to 0$ and the wave becomes purely electrostatic ($\underline{E} \,//\, \underline{k}$).

In the ULF range, the use of (A.24) (A.31) and (A.39) first shows that

$$E_z = 0 \qquad (A.43)$$

which means that the electric field is situated in a plane perpendicular to $\underline{B}$. Second, one has

$$\rho_{\pm} = i \frac{2X\cos\theta}{\sin^2\theta \mp \sqrt{\sin^4\theta + 4X^2\cos^2\theta}} \qquad (A.44)$$

where the upper (or lower) signs have to be used simultaneously. In the QT approximation (X or $\cos\theta$ very small), one finds

$$\rho_- = i \frac{X\cos\theta}{\sin^2\theta} \qquad (A.45)$$

which means that $|E_2/E_1|$ is very small, i.e. that the polarization ellipse (for $\underline{E}$) is much elongated along the x axis. The ellipticity decreases when X or $\cos\theta$ increases. This mode (which is called the slow mode since $W_- < V_A$) is left handed. In the QL approximation

$$\rho_- = i \frac{X\cos\theta}{X\cos\theta + \frac{1}{2}\sin^2\theta} \qquad (A.46)$$

* *Storey computed the angle between axis 1 and the trace of the polarization plane on the xz plane. Let S be this angle. He found* $\tan S = E_3/E_1 = -\tan\theta$, *whereas equation (A.42) shows that* $\tan S = \sin\theta/(x-\cos\theta)$ *where use has been made of the relation* $S = \psi - (\theta + \pi/2)$.

If $\sin^2\theta \ll 2X\cos\theta$, the QL condition (A.13) is a fortiori satisfied so that (A.46) is valid, and

$$\rho_- \sim i \qquad (A.47)$$

The wave is almost circularly polarized in the left hand mode. For $\theta$ strictly equal to 0, equation (A.44) shows that $\rho_-$ is strictly equal to i, so that the wave is strictly circularly polarized.

The deformation of the polarization ellipse when $\theta$ varies from 90° to 0° is shown on Figure A.4. Equivalent drawing can be made for the fast mode ($W_+$) by making use of the fact that $\rho_+\rho_- = 1$ (equation (A.40)).

The displacement of the plasma which is associated with the wave is easily deduced in the low frequency regime (the displacement currents and induction electric fields being negligible) since one has

$$\underline{E} + \underline{v} \times \underline{B} = 0 \qquad (A.48)$$

One is therefore able to deduce the characteristics of the ellipse which is described by the extremity of the velocity vector. For the slow mode ($W_-$) this ellipse is elongated along the y axis so that $\underline{v}$ is almost perpendicular to $\underline{k}$. The mode is said to be 'torsional'. For the fast mode ($W_+$) the ellipse is elongated along the x axis, so that the velocity has a strong component along $\underline{k}$, except for $\theta = 0$. The mode is said to be 'compressional'.

The main propagation and polarization properties of the ULF waves, which are at the origin of their different names, are summarized in Table A.1.



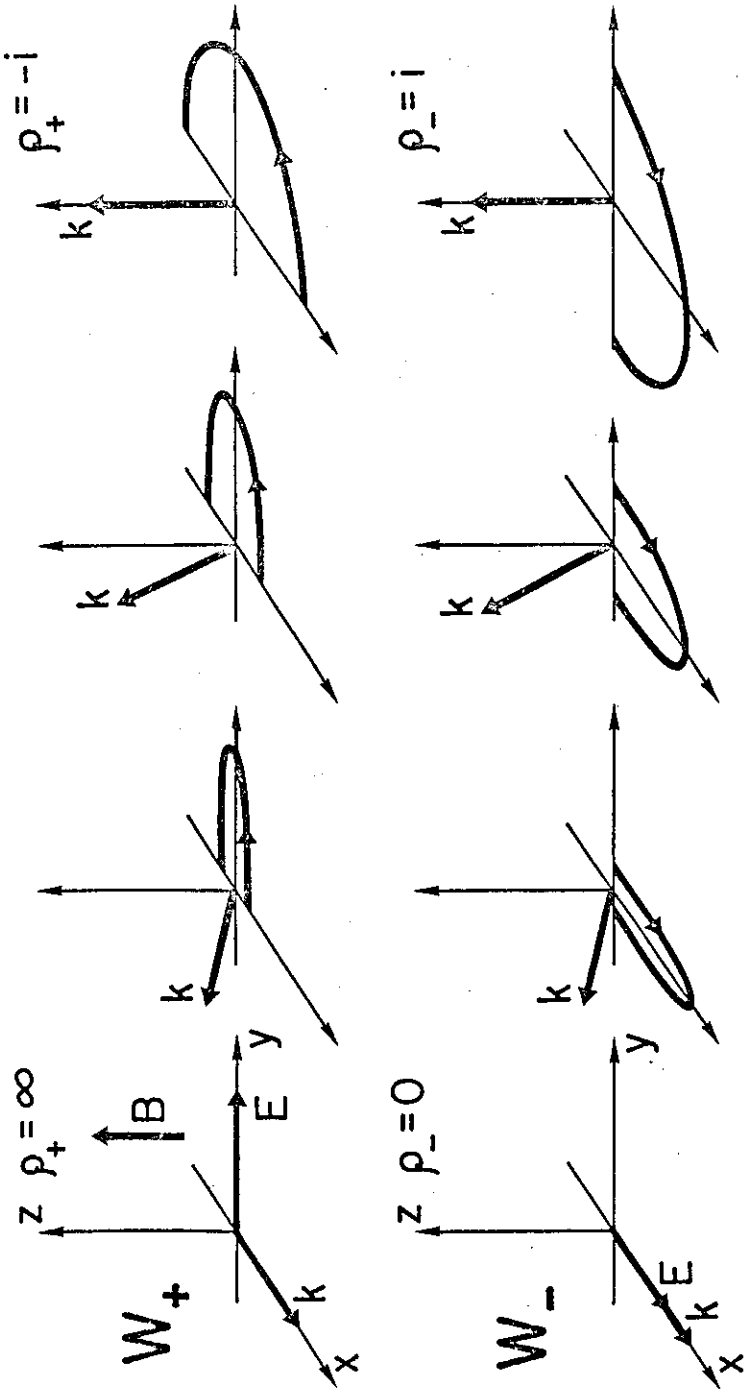


Fig. A.4. Polarization ellipses in the ULF range
For a given wave normal direction, the ellipticity decreases when the frequency increases.

TABLE A.1

Characterization of the two Alfven waves

| Alfven | | Modified Alven | |
|---|---|---|---|
| Fast<br>Isotropic | $(W_+ = V_A)$ | Slow<br>Anisotropic | $(W_- = V_A\cos\theta)$ |
| Right-handed ($\rho_+ \propto -i$) | | Left-handed | ($\rho_- \propto i$) |
| Compressional ($\underline{v}.\underline{k}$ large) | | Torsional | ($\underline{v}.\underline{k}$ small) |

One must note that the equations (A.43) to (A.47) are valid not only when $\alpha^2 = f_{pe}^2/f_{ce}^2 \gg 1$ but also when $f_{pi}^2/f_{ci}^2 \gg 1$ ($\alpha^2 \gg 1/m^*$) which is a less constraining condition.

## A.5. Role of the collisions

All formulas given in this Appendix are valid for a cold plasma without collisions. When collisions exist it is sufficient to replace the particle masses $m_h$ by an 'effective' mass $m_h(1-iZ_h)$ with $Z_h = \nu_h/\omega$ where $\nu_h$ is the collision frequency for the h species. This is due to the fact that in the momentum equation

$$m \frac{\partial \underline{v}}{\partial t} = q\,(\underline{E} + \underline{v} \times \underline{B}) \qquad (A.49)$$

a friction term has to be introduced. This leads to

$$m \frac{\partial \underline{v}}{\partial t} = q\,(\underline{E} + \underline{v} \times \underline{B}) - \nu m \underline{v} \qquad (A.50)$$

which is equivalent to (A.49) if one replaces m by $m\,(1-i\nu/\omega)^*$.

* *This transformation is valid when one considers fields varying like exp(iωt). Sometimes one finds in the literature an opposite convention which leads to an effective mass $m(1+i\nu/\omega)$.*



We must therefore replace $X_h$ by $X_h(1-iZ_h)^{-1}$ and $Y_h$ by $Y_h(1-iZ_h)^{-1}$. This correction is unimportant in the magnetosphere and in the upper ionosphere because the collision frequencies are much smaller than any gyrofrequency. The situation is different in the lower ionosphere, and this correction can even change completely the refraction index and the polarization figure (see Sections 2.2. and section 3. .).

On the contrary temperature effects are always important when one approaches a resonance. The definition of a cold plasma is that the particle thermal velocities are negligible with respect to the phase velocity of the wave. Obviously this condition is not satisfied near a resonance (see Section 3. .). The consequences of this effect are studied in the review by Ginzburg and Ruhadze (1970).